

Fig. 7. Scheme of the hyperthermia experiment for the LNCap group, indicating the various patterns of RH among the five mice. The RH was repeated two or three times.

new hyperthermic procedure, we applied it whether RH could induce the CR of human prostate cancer cell lines (PC-3 and LNCap) in nude mice models. CR was induced in all the tumors in the PC-3 and LNCap groups (Figs. 6 and 8).

PC-3 is a cell line derived from bone metastatic lesions and is androgen-independent [28], whereas LNCap is derived from lymph node metastatic lesions and is androgen-sensitive [29]. In other words, these two prostatic cancer cell lines have different biological characters. In this study, our new hyperthermia method produced CR in all of the tumor nodules in the PC-3 and LNCap groups, although the rates of disappearance differed. In the LNCap group, linear

involution started after just one round of RH, with CR occurring after one to three rounds of RH (Figs. 7 and 8). The PC-3 cancer nodules exhibited greater resistance to hyperthermia. In many cases of the PC-3 group, hyperthermia had no effect on tumor nodules during the first and second rounds, with the last tumors starting involution and exhibiting sudden CR after several RH rounds. This resulted in the total amount of RH rounds being greater for the PC-3 group than for the LNCap group (Figs. 5 and 6). The differing hyperthermic effects between PC-3 and LNCap can be explained as follows: when cultured at 43°C, the PC-3 cell population decreased according to cell-growth inhibition, whereas the LNCap cell population decreased according to a cell-killing effect. This difference is attributable to PC-3 cells possessing heat resistance in which hyperthermic stimulation stops the cell cycle, whereas LNCap cells are more sensitive to hyperthermia because the cell cycle does not change [30]. The huge variation in the time until CR (15–60 days in PC-3, 7–42 days in LNCap: Figs. 6 and 8) can be explained as follows: The distribution of magnetite nanoparticles within tumors must be considered in our use of a hyperthermia system to heat MCLs. When the MCLs were heated, the surrounding tumor tissues underwent necrosis, and magnetite nanoparticles subsequently expanded into the necrotic area within the tumor, resulting in a wide distribution of magnetite nanoparticles [21–23]. In the present study, CR of human prostate cancer cell nodules in nude mice was observed using a hyperthermia protocol, which should in fact be termed frequent RH. For LNCap in mouse 5, it took five rounds of RH to achieve CR. Although parts of the tumor containing sufficient amounts of MCLs were killed by heat, other parts of the tumor without MCLs—

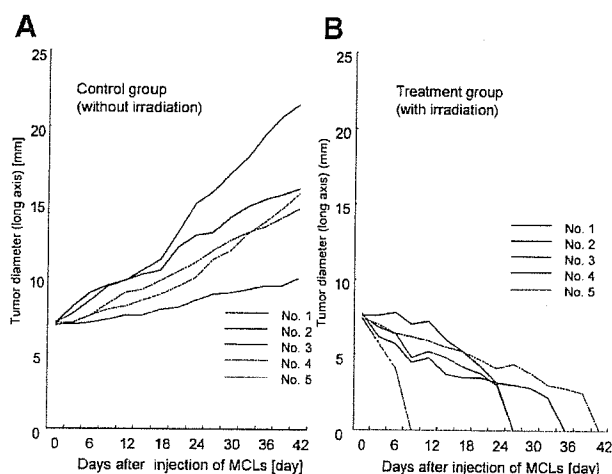


Fig. 8. Tumor long axis of the LNCap group in both the control group (A) and the treatment group (B). Tumor size increased linearly in the control group. However, a linear decrease and CR were demonstrated in the treatment group.

particularly at the tumor edges—may continue to grow. Therefore, differences in the number of rounds of RH treatment for CR are probably due to variations in the tumor shape.

It is well known that there is no reliable therapy for hormone-refractory prostate cancer [31,32]. The use of frequent RH in the present study resulted in CR of PC-3 tumor nodule, which are androgen-independent. This result suggests that frequent RH could be used as one of treatment for hormone-refractory prostate cancer. Since our new hyperthermia technique can induce CR in cancer tissue only by heating, it may be a useful therapy in various types of cancer. From the perspective point of view for clinical use, our new MCL-induced hyperthermia technique will be especially useful if irradiation with an AMF in the FCIS can adequately increase the temperature of tumor tissue injected with MCLs positioned 50 mm above the surface of the coil. The major tumor mass is peripheral in location in clinical stage T2 carcinomas and in 85% of nonpalpable tumors diagnosed on needle biopsy (stage T1c) [33–35], and can be heated by an FCIS attached to the perineal portion since the magnetic flux reaches the peripheral zone of the prostate. In the remaining cases, tumors are predominantly located in the transition zone, and adenocarcinoma of the prostate is multifocal in more than 85% of cases [34]. The development of an endoscopic AMF-generation machine would enable tumors in the transition zone and other multifocal tumors to be treated. The further development of the FCIS will allow our new MCL-induced hyperthermia technique to become a new treatment method for hormone-refractory prostate cancer.

ACKNOWLEDGMENTS

This work was partially supported by a Grant-in-Aid for Scientific Research (No. 13853005), University Start-Ups Creation Support System, and the 21st Century COE Program "Nature-Guided Materials Processing" from the Ministry of Education, Culture, Sports, Science, and Technology of Japan.

REFERENCES

- Levi F, Lucchini F, Negri E, Boyle P, La Vecchia C. Changed trends of cancer mortality in the elderly. *Ann Oncol* 2001;12:1467–1477.
- Littrup PJ. Future benefits and cost-effectiveness of prostate carcinoma screening. *American Cancer Society. Cancer* 1997;80:1864–1870.
- Smart CR. The results of prostate carcinoma screening in the U.S. as reflected in the surveillance, epidemiology, and end results program. *Cancer* 1997;80:1835–1844.
- Schellhammer PF. Editorial: Improving outcomes for primary and salvage therapy of localized prostate cancer. *J Urol* 2003;170:1841–1842.
- Akaza H, Homma Y, Okada K, Yokoyama M, Moriyama N, Usami M, Hirao Y, Tsushima T, Ohashi Y, Aso Y. Early results of LH-RH agonist treatment with or without chlormadinone acetate for hormone therapy of naive localized or locally advanced prostate cancer: A prospective and randomized study. *The Prostate Cancer Study Group. Jpn J Clin Oncol* 2000;30:131–136.
- Han KR, Cohen JK, Miller RJ, Pantuck AJ, Freitas DG, Cuevas CA, Kim HL, Lugg J, Childs SJ, Shuman B, Jayson MA, Shore ND, Moore Y, Zisman A, Lee JY, Ugarte R, Mynderse LA, Wilson TM, Sweat SD, Zinck eH, Belldegrun AS. Treatment of organ confined prostate cancer with third generation cryosurgery: Preliminary multicenter experience. *J Urol* 2003;170:1126–1130.
- Chin JL, Touma N, Pautler SE, Guram KS, Bella AJ, Downey DB, Moussa M. Serial histopathology results of salvage cryoablation for prostate cancer after radiation failure. *J Urol* 2003;170:1199–1202.
- Johnson DB, Nakada SY. Cryoablation of renal and prostate tumors. *J Endourol* 2003;17:627–632.
- Rouviere O, Lyonnet D, Radiant A, Colin-Pan gaud C, Chapelon JY, Bouvier R, Dubernard JM, Gelet A. MRI appearance of prostate following transrectal HIFU ablation of localized cancer. *Eur Urol* 2001;40:265–274.
- Gelet A, Chapelon JY, Bouvier R, Pangaud C, Lasne Y. Local control of prostate cancer by transrectal high intensity focused ultrasound therapy: Preliminary results. *J Urol* 1999;161:156–162.
- Van Leenders GJ, Beerlage HP, Ruijter ET, de la Rosette JJ, van de Kaa CA. Histopathological changes associated with high intensity focused ultrasound (HIFU) treatment for localised adenocarcinoma of the prostate. *J Clin Pathol* 2000;53:391–394.
- Van der Zee J. Heating the patient: A promising approach? *Ann Oncol* 2002;13:1173–1184.
- Abe M, Hiraoka M, Takahashi M, Egawa S, Matsuda C, Onoyama Y, Morita K, Kakehi M, Sugahara T. Multi-institutional studies on hyperthermia using an 8-MHz radiofrequency capacitive heating device (Thermotron RF-8) in combination with radiation for cancer therapy. *Cancer* 1986;58:1589–1595.
- Kroeze H, van de Kamer JB, de Leeuw AA, Kikuchi M, Lagendijk JJ. Treatment planning for capacitive regional hyperthermia. *Int J Hyperthermia* 2003;19:58–73.
- Sherar MD, Gertner MR, Yue CK, O'Malley ME, Toi A, Gladman AS, Davidson SR, Trachtenberg J. Interstitial microwave thermal therapy for prostate cancer: Method of treatment and results of a phase I/II trial. *J Urol* 2001;166:1707–1714.
- Tucker RD, Huidobro C, Larson T, Platz CE. Use of permanent interstitial temperature self-regulating rods for ablation of prostate cancer. *J Endourol* 2000;14:511–517.
- Master VA, Shinohara K, Carroll PR. Ferromagnetic thermal ablation of locally recurrent prostate cancer: Prostate specific antigen results and immediate/intermediate morbidities. *J Urol* 2004;172:2197–2202.
- Deger S, Taymoorian K, Boehmer D, Schink T, Roigas J, Wille AH, Budach V, Wernecke KD, Loening SA. Thermoradiotherapy using interstitial self-regulating thermoseeds: An intermediate analysis of a phase II trial. *Eur Urol* 2004;45:574–579.
- Moroz P, Jones SK, Gray BN. Magnetically mediated hyperthermia: Current status and future directions. *Int J Hyperthermia* 2002;18:267–284.

20. Shinkai M, Yanase M, Honda H, Wakabayashi T, Yoshida J, Kobayashi T. Intracellular hyperthermia for cancer using magnetite cationic liposomes: In vitro study. *Jpn J Cancer Res* 1996;87:1179-1183.
21. Yanase M, Shinkai M, Honda H, Wakabayashi T, Yoshida J, Kobayashi T. Intracellular hyperthermia for cancer using magnetite cationic liposomes: Ex vivo study. *Jpn J Cancer Res* 1997;88:630-632.
22. Yanase M, Shinkai M, Honda H, Wakabayashi T, Yoshida J, Kobayashi T. Intracellular hyperthermia for cancer using magnetite cationic liposomes: An in vivo study. *Jpn J Cancer Res* 1998;89:463-469.
23. Yanase M, Shinkai M, Honda H, Wakabayashi T, Yoshida J, Kobayashi T. Antitumor immunity induction by intracellular hyperthermia using magnetite cationic liposomes. *Jpn J Cancer Res* 1998;89:775-782.
24. Kawai N, Ito A, Nakahara Y, Futakuchi M, Shirai T, Honda H, Kobayashi T, Kohri K. Anticancer effect of hyperthermia on prostate cancer mediated by magnetite cationic liposomes and immune-response induction in transplanted syngeneic rats. *Prostate* 2005;64:373-381.
25. Shinkai M, Ueda K, Ohtsu S, Honda H, Kobayashi T. Effect of functional magnetite particles on frequency capative heating. *Japanese Journal of Cancer Research* 1999; 90:699-704.
26. Cetas TC, Gross EJ, Contractor Y. A ferrite core/metallic sheath thermoseed for interstitial thermal therapies. *IEEE Transactions on Biomedical Engineering* 1998;45:68-77.
27. Ito A, Tanaka K, Honda H, Abe S, Yamaguchi H, Kobayashi T. Complete regression of mouse mammary carcinoma with a size greater than 15 mm by frequent repeated hyperthermia using magnetite nanoparticles. *J Biosciences and Bioengineering* 2003; 4:364-369.
28. Kaighn ME, Narayan KS, Ohnuki Y, Lechner JF, Jones LW. Establishment and characterization of a human prostatic carcinoma cell line (PC-3). *Invest Urol* 1979;17:16-23.
29. Horoszewicz JS, Leong SS, Kawinski E, Karr JP, Rosenthal H, Chu TM, Mirand EA, Murphy GP. LNCaP model of human prostatic carcinoma. *Cancer Res* 1983;43:1809-1818.
30. Nakanoma T, Ueno M, Iida M, Hirata R, Deguchi N. Effects of quercetin on the heat-induced cytotoxicity of prostate cancer cells. *Human cell* 2001;11:623-630.
31. Kasamon KM, Dawson NA. Update on hormone-refractory prostate cancer. *Curr Opin Urol* 2004;14:185-193.
32. Deutsch E, Maggiorella L, Eschwege P, Bourhis J, Soria JC, Abdulkarim B. Environmental, genetic, and molecular features of prostate cancer. *Lancet Oncol* 2004;5:303-313.
33. McNeal JE. Origin and development of carcinoma in the prostate. *Cancer* 1969;23:24-34.
34. Byar DP, Mostofi FK. Carcinoma of the prostate: Prognostic evaluation of certain pathologic features in 208 radical prostatectomies. Examined by the step-section technique. *Cancer* 1972; 30:5-13.
35. Epstein JI, Walsh PC, Carmichael M, Brendler CB. Pathologic and clinical findings to predict tumor extent of non palpable (stage T1c) prostate cancer. *JAMA* 1994;271:368-374.

LETTERS

Topical drug rescue strategy and skin protection based on the role of *Mclr* in UV-induced tanning

John A. D'Orazio^{1,2,3}, Tetsuji Nobuhisa^{1,2}, Rutao Cui^{1,2}, Michelle Arya^{1,2}, Malinda Spry³, Kazumasa Wakamatsu⁴, Vivien Igras^{1,2}, Takahiro Kunisada⁵, Scott R. Granter^{1,6}, Emi K. Nishimura^{1,2,7}, Shosuke Ito⁴ & David E. Fisher^{1,2}

Ultraviolet-light (UV)-induced tanning is defective in numerous 'fair-skinned' individuals, many of whom contain functional disruption of the melanocortin 1 receptor (MC1R)^{1–3}. Although this suggested a critical role for the MC1R ligand melanocyte stimulating hormone (MSH) in this response, a genetically controlled system has been lacking in which to determine the precise role of MSH–MC1R. Here we show that ultraviolet light potently induces expression of MSH in keratinocytes, but fails to stimulate pigmentation in the absence of functional MC1R in red/blonde-haired *Mclr*^{elc} mice. However, pigmentation could be rescued by topical application of the cyclic AMP agonist forskolin, without the need for ultraviolet light, demonstrating that the pigmentation machinery is available despite the absence of functional MC1R. This chemically induced pigmentation was protective against ultraviolet-light-induced cutaneous DNA damage and tumorigenesis when tested in the cancer-prone, xeroderma-pigmentosum-complementation-group-C-deficient genetic background. These data emphasize the essential role of intercellular MSH signalling in the tanning response, and suggest a clinical strategy for topical small-molecule manipulation of pigmentation.

Fair-skinned individuals have an increased incidence of skin cancer and often exhibit weak tanning responses⁴. Although multiple signalling pathways affect melanin production^{5,6}, 'fair' pigmentation in humans is largely the result of sequence variants in *MC1R*—encoding the receptor for MSH^{1,7,8}—that generate weak ligand-induced cAMP responses². Deficient tanning in *MC1R* variant individuals is consistent with a critical role for MSH/cAMP in this response³, but some studies have indicated that melanocyte-directed DNA damage might mediate UV-induced pigmentation^{9,10}. We compared UV tanning responses of wild-type C57BL/6 mice with an intact MSH pathway (*Mclr*^{E/E}) to those of animals possessing an inactivating mutation of the MSH receptor (*Mclr*^{elc}, formerly known as *extension*), the homologue of a gene implicated in having fair skin in humans. Whereas UV-induced hyperpigmentation was grossly and microscopically observed in the ears of control mice, *Mclr*^{elc} (blonde-haired/pheomelanotic) mice lacked detectable pigmentation changes (Fig. 1a) despite comparable melanocyte numbers (Supplementary Fig. 1a). Murine pinnae (external ears) resemble human skin because of the presence of epidermal melanocytes that are lacking in truncal/fur skin.

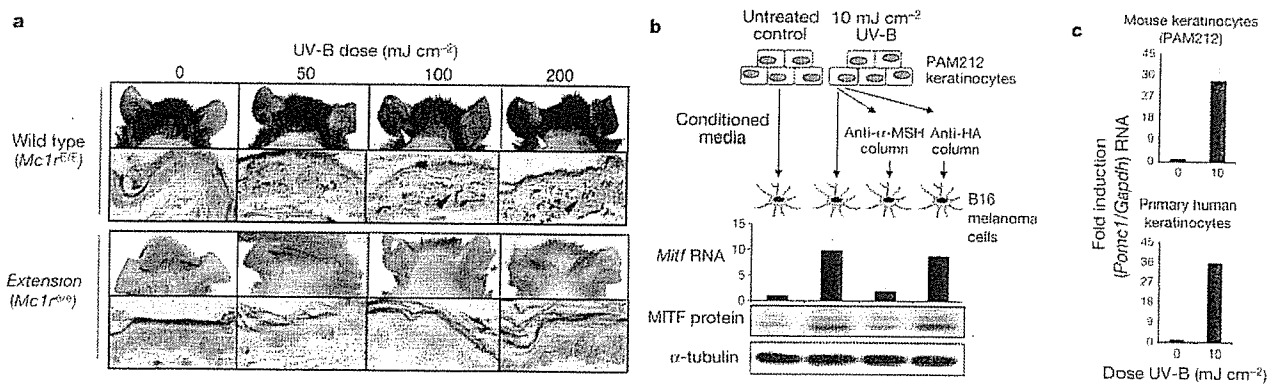


Figure 1 | UV-induced tanning requires an intact MSH pathway. **a**, C57BL/6 mice, either wild-type (*Mclr*^{E/E}) or mutant (*Mclr*^{elc}) at the MSH receptor, were treated five days per week with daily UV-B delivered by a double bank of UV-B lamps (peak emission at 302 nm) for one month. Upper rows show UV-induced ear skin darkening, with corresponding Fontana–Masson-stained skin sections immediately below to show melanin accumulation (black deposits, $\times 400$ magnification). Note the UV-induced skin darkening (white arrows) and melanin accumulation (black arrows) in *Mclr*^{E/E}, but not in *Mclr*^{elc} animals. Although *Mclr*^{elc} skin seems unpigmented, *Dct-LacZ*-tagged transgenic analysis reveals that it contains comparable melanocyte numbers

(Supplementary Fig. 1a). This experiment was repeated with similar results. **b**, *Mitf* induction by qPCR and by western analysis of B16 melanoma cells incubated (6 h) with 24-h conditioned supernatants from mouse keratinocytes either untreated (first lane) or irradiated with 10 mJ cm⁻² UV-B (remaining three lanes). Anti-MSH affinity chromatography (but not control anti-HA) abrogated *Mitf* induction by UV-conditioned media. **c**, qPCR-based detection of *Pomc1* mRNA 6 h after UV irradiation of PAM212 mouse keratinocytes or primary human keratinocytes. All PCR data are reported as fold induction by UV, normalized to *Gapdh* (control); samples were done in triplicate, and the standard deviations (s.d.) between samples are shown.

¹Melanoma Program and ²Department of Pediatric Hematology/Oncology, Dana-Farber Cancer Institute & Children's Hospital, 44 Binney Street, Boston, Massachusetts 02115, USA. ³Department of Pediatrics, Markey Cancer Center and the Graduate Center for Toxicology, University of Kentucky College of Medicine, Lexington, Kentucky 40536, USA. ⁴Department of Chemistry, Fujita Health University, School of Health Sciences, Toyoake, Aichi 470-1192, Japan. ⁵Department of Tissue and Organ Development, Gifu University, Graduate School of Medicine, 1-1 Yanagido, Gifu 501, Japan. ⁶Department of Pathology, Brigham and Women's Hospital, Boston, Massachusetts 02115, USA. ⁷Department of Stem Cell Medicine, Kanazawa University, Cancer Research Institute, 13-1 Takaramachi, Kanazawa 920-0934, Japan.

To examine whether a non-cell-autonomous pathway may mediate the UV pigmentation effect, PAM212 keratinocytes were exposed to UV *in vitro* and culture supernatants were incubated with B16 melanoma cells to test for induction of the microphthalmia transcription factor, MITF¹¹. Media from UV-irradiated (versus non-irradiated) keratinocytes induced MITF messenger RNA and protein in melanoma cells (Fig. 1b). Absorption of conditioned media using anti- α -MSH affinity chromatography removed most of the stimulatory activity, which was not removed with anti-(haemagglutinin) HA. Comparable conditioned media from UV-irradiated murine or primary human melanocytes lacked this activity (Supplementary Fig. 1b). Direct measurements revealed >30-fold induction of *Msh* (otherwise known as pro-opiomelanocortin alpha (*Pomc1*)) expression by UV in PAM212 mouse keratinocytes and primary human keratinocytes (Fig. 1c), whereas <4-fold induction was observed in melanocytes (Supplementary Fig. 1c). These observations corroborate previous findings that UV radiation activates expression of *Msh* in keratinocytes¹². Although melanocytes showed relatively weak UV-induction of *Pomc1* expression, they nonetheless did express some *Pomc1* with or without UV exposure, as previously described^{13,14}, indicating that autocrine signalling could still contribute to MC1R activity.

The UV-unresponsiveness of *Mclr* variants could, in principle, arise from an irreversible block to eumelanin synthesis occurring at some developmental stage. If a cAMP agonist could restore pigmentation in this setting, then the inability of UV to induce pigmentation would be more rigorously linked to inactivity of the cAMP pathway within the *Mclr^{elc}* genetic background. To this end, we used congenic C57BL/6 mice harbouring a transgene in which the keratin 14 promoter drives constitutive expression of stem cell factor (*Scf*; also known as *Kitl*) in the epidermis¹⁵. *K14-Scf* mimics the human

pattern of keratinocyte *SCF* expression as well as epidermal melanocyte homing (the presence of melanocytes in the basal layer of the epidermis), independent of MC1R status (Supplementary Fig. 1d). *K14-Scf* transgenic ('humanized') mice, homozygous for *Mclr^{elc}*, exhibited fair/pink skin with high pheomelanin and low eumelanin content (Supplementary Fig. 2a–c).

Just as in non-transgenic *Mclr^{elc}* mice, we observed no measurable UV-induced melanization in *K14-Scf*-transgenic, *Mclr^{elc}* mice (Fig. 2a; Supplementary Fig. 2d). When forskolin, a cell-permeable diterpenoid that activates adenylyl cyclase¹⁶, was topically applied to *Mclr^{elc}*; *K14-Scf* (pheomelanotic) mice, significant melanization was observed, both when applied throughout (Fig. 2b; Supplementary Fig. 2d) and when applied only to the rump area (Supplementary Fig. 3c). Daily topical forskolin caused progressive and robust darkening (Fig. 2a, Supplementary Fig. 3a), and we conclude that forskolin-induced eumelanization required epidermal melanocytes, because it was not observed in the truncal skin of mice lacking the *K14-Scf* transgene (Supplementary Fig. 3b). Skin darkening by forskolin was associated with dose-dependent accumulation of melanin in the epidermis (Fig. 2c), was progressive over several weeks, and was reversible with a half-life of approximately 2 weeks (Supplementary Fig. 3a). Melanin quantification¹⁷ revealed a >20-fold increase in eumelanin (Fig. 2d) in treated, depilated skin, together with a shift in the eumelanin: pheomelanin ratio from 0.09 ± 0.1 to 0.9 ± 0.5 .

Hair/fur colour was not markedly altered during the time courses examined here. Both crude preparations of forskolin (root extract of *Plectranthus barbatus*, otherwise known as *Coleus forskohlii*)¹⁸ and chemically pure forskolin produced significant melanization (Supplementary Fig. 4a). Importantly, forskolin treatment mimicked melanization to the degree of exhibiting 'nuclear capping', in which

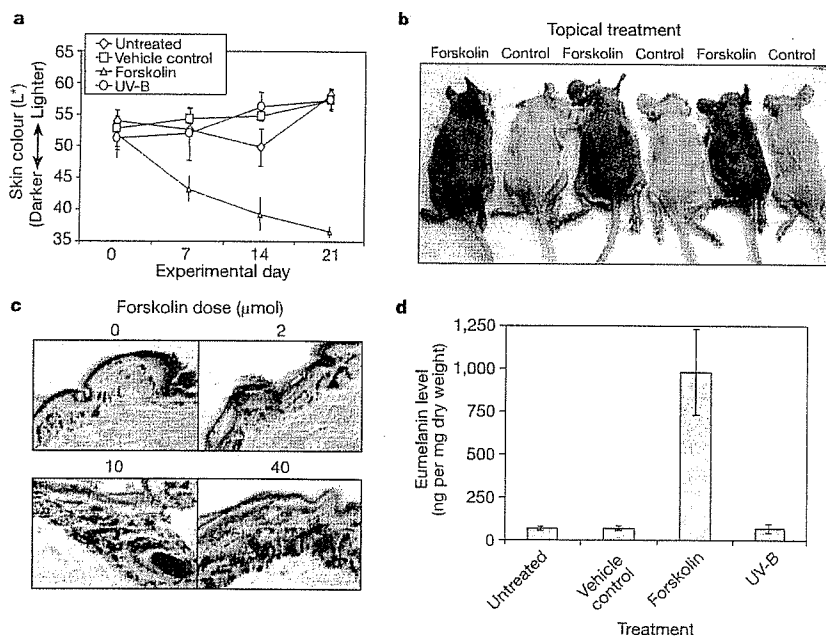


Figure 2 | Forskolin, but not UV, rescues eumelanin production in mice with defective MSH signalling. **a**, Reflective colorimetry measurements (CIE L^* white–black colour axis)²⁹ of skin darkening of *Mclr^{elc}*; *K14-Scf*-transgenic, depilated C57BL/6 mice either topically treated with vehicle control (70% ethanol, 30% propylene glycol), irradiated with 200 mJ cm^{-2} UV-B, topically treated with $400 \mu\text{l}$ of *P. barbatus* root extract (80 μmol forskolin) to the dorsal skin surface for 21 days, or untreated. Lower numbers represent darker skin tones. Skin colour measurements were done in triplicate (different anatomic locations within the treated skin field) and s.d. between

measurements is shown; this experiment was repeated many times with similar results. **b**, Side-by-side photographs of vehicle-control- or forskolin-treated *Mclr^{elc}*; *K14-Scf* animals treated as described in **a**. **c**, Fontana–Masson (eumelanin)-stained skin sections of animals treated for 21 days with the indicated dose of forskolin derived from *P. barbatus* extract ($\times 630$ magnification) as described in **a**. **d**, Eumelanin levels (\pm s.d.) of whole, depilated skin from *Mclr^{elc}*; *K14-Scf* mice treated as described in **a** (ref. 17). Melanin quantification measurements were done in triplicate.

melanosomes exported to keratinocytes align in discrete structures that putatively provide solar shielding to keratinocyte nuclei (Fig. 3a, see asterisks)¹⁹. We conclude that forskolin-induced melanization did not require ectopic SCF because it was also induced on pinnae of non-*K14-Scf* transgenic (C57BL/6) mice (Supplementary Fig. 4c). Collectively, these data demonstrate strong rescue by forskolin of eumelanin production in MC1R-deficient melanocytes, thus indicating that the inability of UV to trigger eumelanization might not be caused by irreversible inactivation of pigmentation machinery.

We considered that small-molecule-induced pigmentation might be UV-protective, so we examined formation of sunburn cells (apoptotic epidermal keratinocytes²⁰) 24 h after a single 200 mJ cm⁻² dose of UV-B (arrows, Fig. 3a). Whereas vehicle-control-treated *Mcl1r^{+/c}* mice were very UV-sensitive, forskolin pre-treatment produced nearly the same degree of UV protection as found in genetically black-skinned (*Mcl1r^{E/E}*) mice (Fig. 3b, c). Tyrosinase mutants (albino) were not protected by forskolin (Fig. 3b, c), suggesting that forskolin-induced keratinocyte survival was mediated by pigmentation, rather than pigment-independent effects. Fluorescence staining for cyclobutane dimers—the mutagenic and most abundant DNA lesion caused by UV-B—revealed dose-dependent nuclear staining at 20 or 50 mJ cm⁻² UV-B in *Mcl1r^{+/c}* and albino (*Tyr^{c2j/c2j}*) skin, but little in *Mcl1r^{E/E}* or forskolin-treated *Mcl1r^{+/c}* mice (Fig. 3c). Forskolin-induced melanization was nearly as protective as *Mcl1r^{E/E}* (genetically black) epidermis.

To test whether forskolin treatment might protect against UV

carcinogenesis, xeroderma-pigmentosum-complementation-group-C-deficient mice (*Xpc^{-/-}*)²¹ were crossed to the fair-skinned *Mcl1r^{+/c}*; *K14-Scf* (C57BL/6 background) mice and subjected to either forskolin-containing or vehicle-control topical treatments for four weeks, before daily exposure to 250 mJ cm⁻² UV-B (along with continued topical treatments) for 20 weeks—a UV dose approximating 1–2 h of ambient midday sun exposure at sea level in Florida, during July (<http://www.srrb.noaa.gov/UV/>). This low-dose chronic UV schedule was chosen for its propensity to induce keratinocyte neoplasms²¹. Vehicle control (non-darkened) mice exhibited gross and histologic evidence of sun damage, including failure to thrive (diminished weight-gain; Supplementary Fig. 5a, b), profound epidermal thickening, and inflammation and scarring (Supplementary Fig. 6a, b). All such damage was significantly prevented by forskolin pretreatment. Following chronic UV, eleven neoplasms developed in the nine vehicle-control, irradiated mice within nine weeks of cessation of UV radiation (Fig. 4a, b), with two of the nine mice developing multiple tumours. As anticipated (by dose and schedule regimen), the majority were squamous cell carcinomas (Fig. 4b). Forskolin pretreatment was significantly protective in delaying onset of UV-induced tumours (median of four weeks in controls versus 25 weeks in forskolin-treated; $P < 0.001$). In all, vehicle-control-treated, irradiated mice developed 11 tumours whereas forskolin-treated, irradiated mice developed six tumours. Given the extreme UV sensitivity of homozygous *Xpc* deficiency, coupled to the high chronic UV doses used, these data suggest a

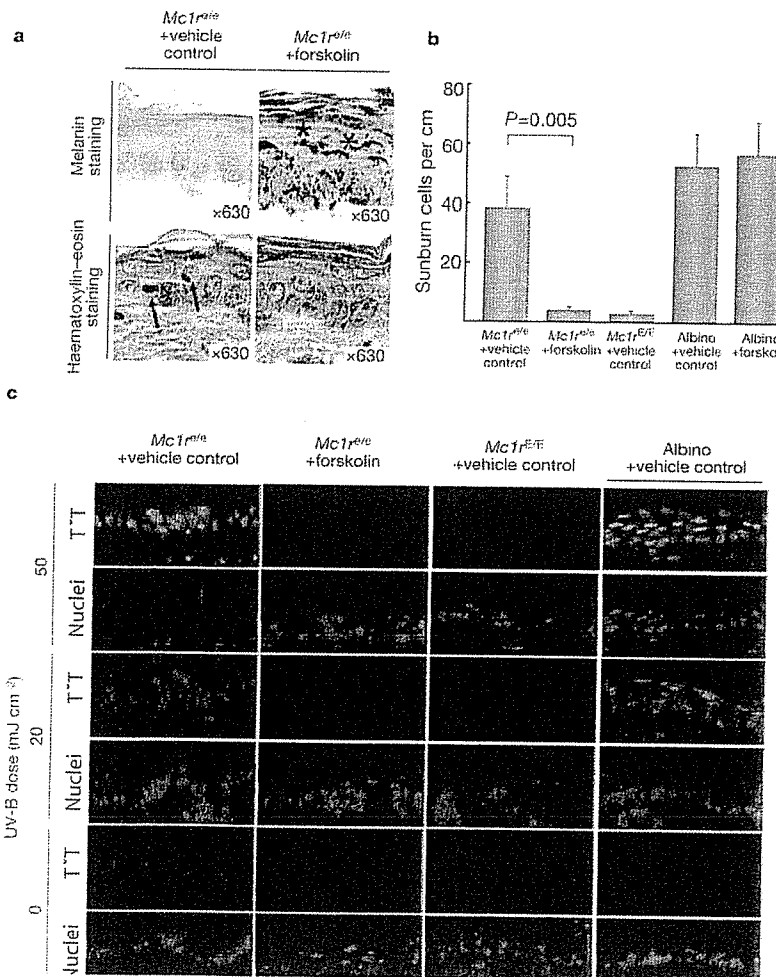


Figure 3 | Forskolin-induced melanin deposition protects against UV-mediated cutaneous damage.

Mcl1r^{+/c}; *K14-Scf*, depilated animals were pretreated for 15 days with either vehicle control or *P. barbatum* root extract (80 μmol forskolin) before exposure to 200 mJ cm⁻² UV-B. **a**, Melanin distribution in the skin 24 h after UV exposure as determined by Fontana–Masson (upper panels) or haematoxylin–eosin staining (lower panels). We note the greatly enhanced deposition of epidermal melanin (black staining) in forskolin-treated animals in a keratinocyte nucleus-capping pattern (see asterisks) and the presence of ‘sunburn cells’, which represent apoptotic keratinocytes in UV-irradiated animals not pre-treated with forskolin (arrows). **b**, Sunburn cell quantification in UV-exposed depilated animals treated as described in **a**. Shown are means ± s.d. of at least three samples per condition. Forskolin pre-treatment of fair-skinned animals yielded as much protection as *Mcl1r^{E/E}* (eumelanotic) animals. Amelanotic (albino) animals had high levels of UV-induced apoptosis regardless of whether they were treated with forskolin before UV exposure, suggesting that forskolin’s protective effect is pigmentation-dependent. **c**, UV-induced thymine dimer formation in depilated skin harvested ten minutes after UV irradiation from *Mcl1r^{+/c}*, *Mcl1r^{E/E}* or *Tyr^{c2j/c2j}* (albino); *K14-Scf* mice pretreated with either vehicle control or *P. barbatum* root extract (80 μmol forskolin). DAPI stain highlights epidermal nuclei (blue), as does thymine-dimer-directed immunofluorescence (T~T, green) in DNA-damaged skin in a dose-dependent fashion. Non-fluorescent (immunohistochemical) staining for pyrimidine dimers revealed the same protection, ruling out potential fluorescence quenching by melanin (Supplementary Fig. 4b). This experiment was repeated at least once with similar results.

significant protection afforded by topical rescue of MC1R functional deficiency.

A requirement for MSH/MC1R signalling in UV-induced pigmentation is plausible, given previous studies of pheomelanin production^{2,3}, agouti signalling protein (a natural MC1R antagonist)²², and UV induction of *Msh* expression in keratinocytes¹². UV also upregulated *MSH* in melanocytes (as previously reported^{13,14}), but it did so to a much smaller degree than in keratinocytes. These studies therefore cannot firmly discriminate the relative roles of keratinocytes versus melanocyte MSH (paracrine versus autocrine) in the observed UV response, and indeed it is possible that both are contributory. Furthermore, the observed essential role of MC1R signalling in the tanning response does not diminish the potential contributions of other pathways. Thus, although forskolin was singularly capable of restoring dramatic melanization, other signalling factors (endothelin-1, β -FGF, NO, SCF, p38, USF and others) have been implicated in the UV adaptive tanning response^{23–28} and it will be valuable to determine their relative contributions.

It will also be important to understand the pathway through which UV induces *Pomc1/Msh* expression in keratinocytes, because it is possible that alterations in *Msh* induction by UV could contribute to cancer risk (for example, in dark-haired, fair-skinned people). Previous work with topical cAMP agonists in other animal models showed that forskolin did not darken light-skinned swine, but did promote histologically identifiable melanin accumulation in the epidermis¹⁶ (although this was not studied in a UV-resistant *Mcl1r* variant background). The greater robustness of the forskolin response in mice may involve a thinner epidermis or genetic features that are ill-defined in swine. Clearly, small-molecule delivery would

need to be optimized before pigmentation in the absence of sun could be successful in humans.

Whereas rescue of eumelanization was observed with topical forskolin, the cAMP agonist effect was not explicitly targeted to melanocytes within the skin. *In vitro* studies showed no measurable melanocytic stimulation from cultured supernatants of forskolin-treated keratinocytes (data not shown). Still, it is theoretically possible that part of the rescue may have involved non-cAMP or pigment-independent effects, or even potential impurities within the small-molecule preparation, although forskolin could not rescue keratinocyte apoptosis in UV-irradiated albinos. The topical rescue of eumelanization confirms the 'availability' of the pigmentation machinery in adults, given appropriate signals. It remains to be seen whether topical melanization will be achievable in man, and whether it would afford measurable protection against UV skin damage and cancer.

METHODS

See Supplementary Information for detailed methods.

Mice. C57BL/6J *Mcl1r^{+/+}*; *Tyr^{+/+}* mice, C57BL/6J *Mcl1r^{+/+}* mice and C57BL/6J *Mcl1r^{+/+}*; *Tyr^{+/+}* mice were crossed with *K14-Scf* transgenic mice¹⁵, dopa-chrome tautomerase (*Dct*)-*LacZ* transgenic mice or *Xpc*-null animals.

Melanization experiments. Depilated animals were exposed to either UV-B with UV-B lamps (UV Products), topical forskolin or vehicle control. Skin reflective colorimetry measurements were assessed with a CR-400 Colorimeter (Minolta) and the degree of melanization was calculated²⁹. Skin biopsies were harvested and processed for Fontana–Masson (eumelanin) staining and melanin quantification¹⁷.

Histology and immunohistochemistry. Skin biopsies were fixed and paraffin-sectioned (haematoxylin–eosin or Fontana–Masson staining) or frozen-sectioned (immunohistochemistry and β -galactosidase staining)³⁰. Immunohistochemistry used an anti-thymine-dimer, monoclonal antibody (Kamiya Biomedical) followed by Alexa-Fluor-488-conjugated, anti-mouse IgG donkey antibody (Molecular Probes).

Quantitative polymerase chain reaction and western blotting. Melanocyte or keratinocyte cells were exposed to UV radiation, anti-MSH or treated cell supernatants as indicated. MSH was neutralized from cell supernatants using anti-MSH (Sigma). MITF detection by western blotting employed the C5 monoclonal antibody³¹. RNA was extracted and *Mitf* mRNA expression was quantified by quantitative Taqman polymerase chain reaction (qPCR) using QuantiTect Probe reverse transcription (RT)-PCR kits (Qiagen).

Tumour formation and chronic UV protection experiments. C57BL/6 *Mcl1r^{+/+}*; *K14-Scf*; *Xpc^{-/-}* animals were irradiated (250 mJ cm⁻² day⁻¹) beginning at seven weeks of age over the course of 20 weeks, after one month's topical pretreatment with either forskolin or vehicle control. Animals were weighed and skin samples were harvested after 16 weeks of irradiation. Animals were then monitored for tumour surveillance over the next 52 weeks. Lesions that were grossly identified as tumours were biopsied and examined.

Received 28 March; accepted 14 July 2006.

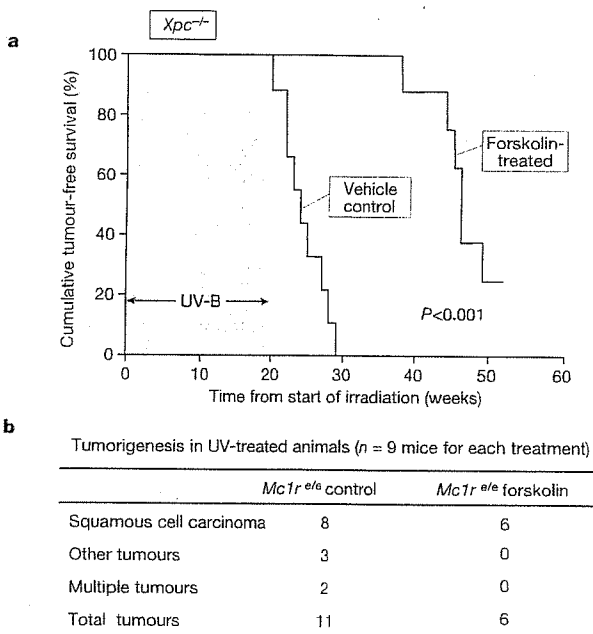


Figure 4 | Protective effect of topical forskolin against chronic UV damage. *K14-Scf* transgenic, *Mcl1r^{+/+}*, depilated animals homozygously deficient for the *Xpc* gene²¹ were pretreated with either vehicle control or topical forskolin and exposed to daily low-dose UV-B for 16–20 weeks. **a**, Kaplan–Meier analysis of tumour incidence in irradiated, vehicle-control-treated versus forskolin-treated, irradiated *Mcl1r^{+/+}*; *K14-Scf*; *Xpc^{-/-}* mice. The yellow bar indicates duration of daily UV exposure. **b**, Tumour subtypes and incidence in vehicle-control-treated versus forskolin-treated, irradiated *Mcl1r^{+/+}*; *K14-Scf*; *Xpc^{-/-}* animals. Some vehicle-control-treated, irradiated animals developed multiple distinct tumours, whereas none of the forskolin-treated animals developed more than one tumour.

- Mountjoy, K. G., Robbins, L. S., Mortrud, M. T. & Cone, R. D. The cloning of a family of genes that encode the melanocortin receptors. *Science* 257, 1248–1251 (1992).
- Valverde, P., Healy, E., Jackson, I., Rees, J. L. & Thody, A. J. Variants of the melanocyte-stimulating hormone receptor gene are associated with red hair and fair skin in humans. *Nature Genet.* 11, 328–330 (1995).
- Rouzaud, F., Kadakara, A. L., Abdel-Malek, Z. A. & Hearing, V. J. MC1R and the response of melanocytes to ultraviolet radiation. *Mutat. Res.* 571, 133–152 (2005).
- Sturm, R. A. et al. Genetic association and cellular function of MC1R variant alleles in human pigmentation. *Ann. NY Acad. Sci.* 994, 348–358 (2003).
- Van Raamsdonk, C. D., Fitch, K. R., Fuchs, H., de Angelis, M. H. & Barsh, G. S. Effects of G-protein mutations on skin color. *Nature Genet.* 36, 961–968 (2004).
- Lamason, R. L. et al. SLC24A5, a putative cation exchanger, affects pigmentation in zebrafish and humans. *Science* 310, 1782–1786 (2005).
- Naysmith, L. et al. Quantitative measures of the effect of the melanocortin 1 receptor on human pigmentation status. *J. Invest. Dermatol.* 122, 423–428 (2004).
- Rees, J. L. The genetics of sun sensitivity in humans. *Am. J. Hum. Genet.* 75, 739–751 (2004).
- Eller, M. S., Yaar, M. & Giichrest, B. A. DNA damage and melanogenesis. *Nature* 372, 413–414 (1994).

10. Eller, M. S., Ostrom, K. & Gilchrist, B. A. DNA damage enhances melanogenesis. *Proc. Natl Acad. Sci. USA* 93, 1087–1092 (1996).
11. Price, E. R. *et al.* α -melanocyte-stimulating hormone signaling regulates expression of *microphthalmia*, a gene deficient in Waardenburg syndrome. *J. Biol. Chem.* 273, 33042–33047 (1998).
12. Wintzen, M., Yaar, M., Burbach, J. P. & Gilchrist, B. A. Proopiomelanocortin gene product regulation in keratinocytes. *J. Invest. Dermatol.* 106, 673–678 (1996).
13. Corre, S. *et al.* UV-induced expression of key component of the tanning process, the *POMC* and *MCTR* genes, is dependent on the p-38-activated upstream stimulating factor-1 (USF-1). *J. Biol. Chem.* 279, 51226–51233 (2004).
14. Chakraborty, A. K. *et al.* Production and release of proopiomelanocortin (POMC) derived peptides by human melanocytes and keratinocytes in culture: regulation by ultraviolet B. *Biochim. Biophys. Acta* 1313, 130–138 (1996).
15. Kunisada, T. *et al.* Murine cutaneous mastocytosis and epidermal melanocytosis induced by keratinocyte expression of transgenic stem cell factor. *J. Exp. Med.* 187, 1565–1573 (1998).
16. Seamon, K. B. & Daly, J. W. Forskolin: a unique diterpene activator of cyclic AMP-generating systems. *J. Cyclic Nucleotide Res.* 7, 201–224 (1981).
17. Wakamatsu, K. & Ito, S. Advanced chemical methods in melanin determination. *Pigment Cell Res.* 15, 174–183 (2002).
18. Lin, C. B. *et al.* Modulation of microphthalmia-associated transcription factor gene expression alters skin pigmentation. *J. Invest. Dermatol.* 119, 1330–1340 (2002).
19. Kobayashi, N. *et al.* Supranuclear melanin caps reduce ultraviolet induced DNA photoproducts in human epidermis. *J. Invest. Dermatol.* 110, 806–810 (1998).
20. Bayerl, C., Taake, S., Moll, I. & Jung, E. G. Characterization of sunburn cells after exposure to ultraviolet light. *Photodermatol. Photoimmunol. Photomed.* 11, 149–154 (1995).
21. Sands, A. T., Abuin, A., Sanchez, A., Conti, C. J. & Bradley, A. High susceptibility to ultraviolet-induced carcinogenesis in mice lacking *XPC*. *Nature* 377, 162–165 (1995).
22. Sakai, C. *et al.* Modulation of murine melanocyte function *in vitro* by agouti signal protein. *EMBO J.* 16, 3544–3552 (1997).
23. Hirobe, T. Basic fibroblast growth factor stimulates the sustained proliferation of mouse epidermal melanoblasts in a serum-free medium in the presence of dibutyryl cyclic AMP and keratinocytes. *Development* 114, 435–445 (1992).
24. Cook, A. L. *et al.* Human melanoblasts in culture: expression of *BRN2* and synergistic regulation by fibroblast growth factor-2, stem cell factor, and endothelin-3. *J. Invest. Dermatol.* 121, 1150–1159 (2003).
25. Lassalle, M. W. *et al.* Effects of melanogenesis-inducing nitric oxide and histamine on the production of eumelanin and pheomelanin in cultured human melanocytes. *Pigment Cell Res.* 16, 81–84 (2003).
26. Grichnik, J. M., Burch, J. A., Burchette, J. & Shea, C. R. The SCF/KIT pathway plays a critical role in the control of normal human melanocyte homeostasis. *J. Invest. Dermatol.* 111, 233–238 (1998).
27. Kadekaro, A. L. *et al.* α -Melanocortin and endothelin-1 activate antiapoptotic pathways and reduce DNA damage in human melanocytes. *Cancer Res.* 65, 4292–4299 (2005).
28. Galibert, M. D., Carreira, S. & Goding, C. R. The *Usf-1* transcription factor is a novel target for the stress-responsive p38 kinase and mediates UV-induced *Tyrosinase* expression. *EMBO J.* 20, 5022–5031 (2001).
29. Park, S. B., Suh, D. H. & Youn, J. I. A long-term time course of colorimetric evaluation of ultraviolet light-induced skin reactions. *Clin. Exp. Dermatol.* 24, 315–320 (1999).
30. Nishimura, E. K., Granter, S. R. & Fisher, D. E. Mechanisms of hair graying: incomplete melanocyte stem cell maintenance in the niche. *Science* 307, 720–724 (2005).

Supplementary Information is linked to the online version of the paper at www.nature.com/nature.

Acknowledgements We thank A. Tsay, J. Du, H. Widlund, M. Seiberg, I. Davis and A. Wagner for discussions and help with technical aspects of the studies; I. Jackson for *Dct-LacZ* mice; S. Yuspa for PAM212 cells; and D. Bennett for Melan-C cells. We also thank the University of Kentucky's Teaching and Academic Support Center (TASC) for help with figure preparation. This work was supported by grants from the NIH (D.E.F.) and the Doris Duke Charitable Foundation. S.I. and K.W. were supported in part by a Grant-in-Aid for Scientific Research from the Ministry of Education, Culture, Sports and Technology of Japan. D.E.F. is the Jan and Charles Nirenberg Fellow in Pediatric Oncology at the Dana-Farber Cancer Institute, and a Doris Duke Distinguished Clinical Investigator.

Author Information Reprints and permissions information is available at www.nature.com/reprints. The authors declare competing financial interests: details accompany the paper at www.nature.com/nature. Correspondence and requests for materials should be addressed to D.E.F. (david_fisher@dfci.harvard.edu).

Diversity of pigmentation in cultured human melanocytes is due to differences in the type as well as quantity of melanin

Kazumasa Wakamatsu¹, Renny Kavanagh², Ana L. Kadekaro², Silva Terzieva², Richard A. Sturm³, Sancy Leachman⁴, Zalfa Abdel-Malek² and Shosuke Ito^{1,*}

¹Department of Chemistry, Fujita Health University School of Health Sciences, Toyoake, Aichi, Japan

²Department of Dermatology, University of Cincinnati College of Medicine, Cincinnati, OH, USA

³Institute for Molecular Bioscience, The University of Queensland, Brisbane, Qld, Australia

⁴Department of Dermatology and Huntsman Cancer Center, University of Utah, Salt Lake City, UT, USA

*Address correspondence to Shosuke Ito,
e-mail: sito@fujita-hu.ac.jp

Summary

Cultured human melanocytes differ tremendously in visual pigmentation, and recapitulate the pigimentary phenotype of the donor's skin. This diversity arises from variation in type as well as quantity of melanin produced. Here, we measured contents of eumelanin (EM) and pheomelanin (PM) in 60 primary human melanocyte cultures (51 neonatal and nine adults), and correlated some of these values with the respective activity and protein levels of tyrosinase, and the *melanocortin-1 receptor (MC1R)* genotype. Melanocytes were classified into four phenotypes (L, L+, D, D+) as depicted by visual pigmentation using light microscopy, and by the pigimentary phenotype of the donor's skin. There were large differences in total melanin (TM) and EM, which increased progressively for L, L+, D and D+ melanocytes. TM content, the sum of EM and PM, showed a good correlation with TM measured spectrophotometrically, and with the activity and protein levels of tyrosinase. Log EM/PM ratio did not correlate with *MC1R* genotype. We conclude that: (i) EM consistently correlates with the visual phenotype; (ii) lighter melanocytes tend to be more pheomelanin in composition than darker melanocytes; (iii) in adult melanocyte cultures, EM correlates with the ethnic background of the donors (African-American > Indian > Caucasian); and (iv) *MC1R* loss-of-function mutations do not necessarily alter the phenotype of cultured melanocytes.

Key words: eumelanin/melanocortin-1 receptor/melanocytes/pheomelanin/tyrosinase

Received 17 October 2005, revised and accepted for publication 5 December 2005

Introduction

Cultured human melanocytes show a tremendous diversity of visual pigmentation, and recapitulate the pigimentary phenotype of the skin from which they were derived (Hunt et al., 1995; Scott et al., 2002). We suggest that this diversity is due to variation in type as well as quantity of melanin produced.

The production of melanin pigment is catalyzed by the specific enzyme tyrosinase, which converts L-tyrosine to dopaquinone (Hearing, 1998; Ito, 2003). Dopaquinone is a highly reactive molecule, and is rapidly cyclized to form dopachrome, which is then either decarboxylated to give 5,6-dihydroxyindole or tautomerized to give 5,6-dihydroxyindole-2-carboxylic acid. These dihydroxyindoles are then oxidized to form eumelanin (EM), a dark brown to black pigment. However, in the presence of cysteine dopaquinone binds to form 5-S-cysteinyl-dopa, along with minor isomers (Ito, 2003). Oxidation of cysteinyl-dopa isomers in melanocytes leads to the production of pheomelanin (PM), a yellow to reddish melanin.

In reality, most of the melanin pigments present in the hair, skin, and eyes are not homopolymers of a single monomer unit, but rather they are complex heteropolymers made up of both EM and PM building blocks (Ito, 1997; Ito and Wakamatsu, 2003; Liu et al., 2005; Protá, 1992). Thus, the color of human skin, hair, and eyes should reflect not only the type of melanin produced but also the quality of melanin, i.e. EM/PM ratio (Ito and Wakamatsu, 2003). In fact, hair color determined objectively using the $L^*a^*b^*$ color system correlated well with melanin contents (Naysmith et al., 2004). Thus, the log values of EM/PM ratio were inversely related to the color variables b^* (yellow–blue), a^* (red–green), and to a lesser extent L^* (light–dark). Moreover, recent studies on human skin show that total melanin (TM) and EM and PM contents correlated with skin color measured on the L^* scale (Alaluf et al., 2002;

Hennessy et al., 2005). However, studies on cultured human melanocytes measuring EM and PM contents have been only sporadic with limited numbers of cultures tested (De Leeuw et al., 2001; Hunt et al., 1995; van Nieuwpoort et al., 2004; Scott et al., 2002; Smit et al., 1998).

The *melanocortin-1 receptor (MC1R)* gene encodes a G-protein coupled receptor that is primarily expressed on melanocytes, where it plays a key role in pigmentation regulation, and some variant alleles are associated with red hair color (RHC) and fair skin, as well as skin cancer risk (Beaumont et al., 2005; García-Borrón et al., 2005; Rees, 2003). Reduction in receptor coupling as well as cell surface localization appears to be the major factor to the genetic association between the MC1R variants and the RHC phenotype. The role of MC1R in pigmentation regulation in cultured melanocytes has been investigated in the present study.

To evaluate the tremendous diversity of visual pigmentation in cultured human melanocytes, we measured contents of EM and PM in 60 primary human melanocyte cultures, and correlated some of these values with visual pigmentation, activity and protein levels of tyrosinase, and with *MC1R* genotype. Contents of EM and PM (chemical phenotype) were determined by high-performance liquid chromatography (HPLC) microassays (Wakamatsu and Ito, 2002). This represents the largest study on pigmentation in cultured human melanocytes and has led to the conclusion that EM, but not always PM, consistently correlates with the visual pigmentation (visual phenotype).

Results

Primary cultures of human melanocytes

A summary of primary cultures of human melanocytes used in this study is shown in Table 1. We examined 60 primary cultures isolated from 51 neonatal and nine adult skins. Those melanocytes were classified into four types: L (very light), L+ (light), D (fairly dark), and D+ (dark) lines, based on pigmentation depicted by light microscopic observation and the pigmentation of donors' skin. In this report, we propose to call this clas-

Table 1. Classification of cultured human melanocytes based on visual pigmentation

n	Classification	Visual pigmentation	Number of melanocyte cultures		
			Total	Neonatal	Adult
1–28	L	Very light	28	26	2
29–41	L+	Light	13	11	2
42–48	D	Fairly dark	7	7	0
49–60	D+	Dark	12	7	5

sification visual phenotype. Photographs of representative cultures are shown in Figure 1. Most of melanocytes were dipolar in shape regardless of the visual phenotype and differ only in pigmentation.

Correlation of EM and PM contents with visual pigmentation

We measured contents of EM and PM (chemical phenotype) in the 60 primary cultures using our HPLC methods. As shown in Figure 2, there was a great diversity in TM contents measured as the sum of EM and PM among different cultures. Thus, TM levels (mean \pm SE) increased progressively and significantly ($P < 0.005$) from 5.8 ± 0.7 , 29 ± 3.6 , 50 ± 4.4 to $126 \pm 19 \mu\text{g}/10^6$ cells for L, L+, D, and D+ cells, respectively. Distribution of EM and PM values were rather skewed, and thus those values were next compared in log scale. Log EM levels ($\mu\text{g}/10^6$ cells) increased steeply and highly significantly ($P < 0.0001$) from 0.34 ± 0.06 , 1.25 ± 0.05 , 1.59 ± 0.04 to 1.96 ± 0.05 (Figure 3A), while log PM levels ($\mu\text{g}/10^6$ cells) increased more gradually from 0.31 ± 0.08 , 0.74 ± 0.14 , 0.89 ± 0.15 to 1.26 ± 0.11 for L, L+, D, and D+ cells, respectively ($P < 0.01$ for L versus other phenotypes, Figure 3B). Thus, log PM levels were more variable than log EM levels. Log EM/PM ratios also showed an increase from 0.03 ± 0.05 , 0.52 ± 0.15 , to 0.71 ± 0.15 for L, L+, and D cells, respectively ($P < 0.005$ for L versus other phenotypes, Figure 3C). Log EM/PM ratio did not increase in D+ cells (0.70 ± 0.11) compared with D cells. These results indicate that lighter melanocytes tend to be more pheomelanin in composition than darker melanocytes. However, there were great diversities in the log EM/PM ratios within the same visual phenotypes as well, as illustrated in Figures 2 and 3C.

We examined whether TM content, representing the sum of EM and PM, correlates well with TM measured by spectrophotometry. For this purpose, we randomly selected 24 cell cultures having a diverse degree of pigmentation. As shown in Figure 4, TM content measured by HPLC showed a good correlation ($R^2 = 0.913$) with TM content measured spectrophotometrically in the 24 cell cultures.

In nine adult melanocyte cultures (Figure 2), the chemical phenotype correlated well with the ethnic background of the donors: four Caucasians had the least (mean EM levels $8.9 \mu\text{g}/10^6$ cells), two Indians had more ($68 \mu\text{g}/10^6$ cells), and three African-Americans had the highest EM ($156 \mu\text{g}/10^6$ cells). Interestingly, adult melanocyte cultures appeared to be more pheomelanin as compared with neonatal melanocyte cultures, with a difference in log PM levels between nine adult and 51 neonatal cultures being highly significant ($P < 0.0001$). Furthermore, between seven adults and 25 neonatal cultures with darker phenotypes (L+, D, and D+), their log EM/PM ratio also showed a significant difference ($P < 0.05$) as did the log PM ($P < 0.0001$).

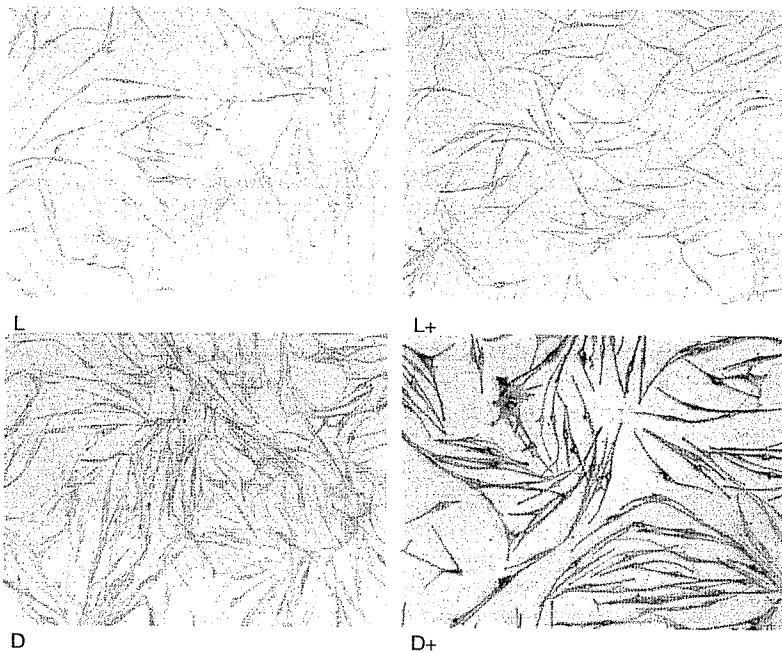


Figure 1. Photographs of cultured human melanocytes classified into the four phenotypes on the basis of visual pigmentation (see Table 1).

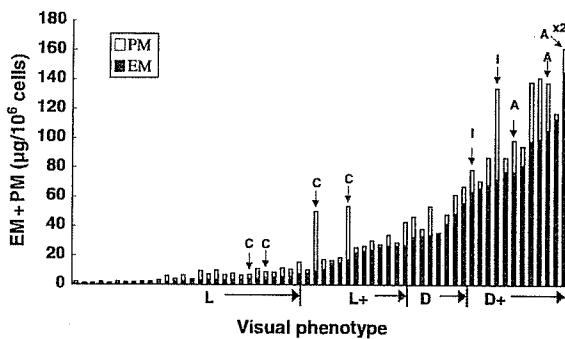


Figure 2. Contents of eumelanin (EM) and pheomelanin in the 60 melanocytes cultures examined. They were classified into the four visual phenotypes based on visual pigmentation (see Table 1) and shown in the sequence of increasing amount of EM in each phenotype group. Bars with arrow denote melanocyte cultures from adult skin biopsies: C, Caucasian; I, Indian; A, African-American; x2 indicates that actual values are twice those shown.

Correlation of TM content with tyrosinase activity and protein level

Total melanin content, measured as the sum of EM and PM, was compared with tyrosinase activity as well as tyrosinase protein level. As shown in Figure 5A, TM content correlated well ($R^2 = 0.782$) with tyrosinase activity in the randomly selected 12 cell cultures with different visual pigmentation, and the differences in TM and tyrosinase activity between the lightest and darkest cultures approached 50-fold. On the other hand, when the same cultures were analyzed for protein levels of tyrosinase by Western blotting (Figure 5B), the

differences in tyrosinase level were not as dramatic as those in TM content and tyrosinase activity.

Correlation of EM/PM ratio with MC1R variation

We analyzed 19 selected cultures, nine of which were previously investigated in an earlier study (Scott et al., 2002), for *MC1R* genotype and the ability to respond to α -melanocyte stimulating hormone (α -MSH) with increased cAMP formation, proliferation, tyrosinase activity, reduction in UV-induced apoptosis and hydrogen peroxide generation, and enhanced repair of DNA photoproducts, as described by Scott et al. (2002) and Kadarkar et al. (2005). We found that melanocytes with loss-of-function *MC1R* due to expression of various *MC1R* alleles (Table 2) did not show striking differences in their log EM, log PM, or log EM/PM ratio from melanocytes with functional *MC1R* ($P > 0.05$). Thus, loss-of-function mutations of *MC1R* failed to show a correlation with the chemical phenotype. This was particularly true for one culture (no. 32) that had a high EM (and a low PM), despite expressing two strong 'red hair' alleles (R151C/D294H). Other melanocytes with loss-of-function *MC1R* had mostly low EM and PM values, which were comparable with those of melanocytes with functional *MC1R*.

Discussion

Cultured human melanocytes show a tremendous diversity of visual pigmentation (visual phenotype). The aim of this study was to evaluate the effects of EM and PM contents (chemical phenotype), activity and protein level of tyrosinase, and *MC1R* mutations on the visual

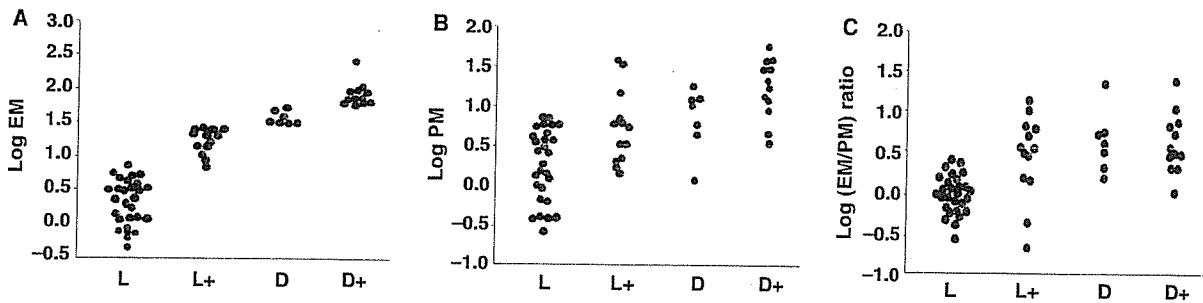


Figure 3. Chemical phenotype in relation to visual phenotype in the 60 cultures. Melanocytes were classified into the four visual phenotypes based on visual pigmentation (see Table 1). (A) Log eumelanin (EM) levels ($\mu\text{g}/10^6$ cells) in relation to visual phenotype. $P < 0.0001$ for any pair of the phenotypes. (B) Log pheomelanin (PM) levels ($\mu\text{g}/10^6$ cells) in relation to visual phenotype; $P < 0.01$ for pairs of L vs L+, D, or D+, and L+ vs D+. (C) Log EM/PM ratio in relation to visual phenotype; $P < 0.005$ for pairs of L vs L+, D, or D+.

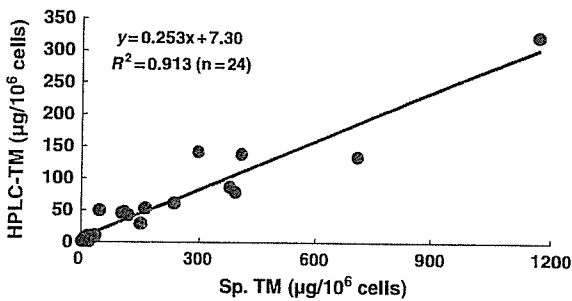


Figure 4. Correlation between total melanin (TM) content as the sum of eumelanin and pheomelanin, and TM content as measured spectrophotometrically.

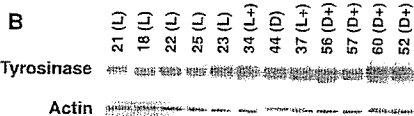
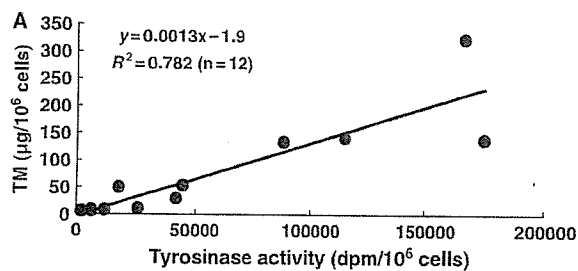


Figure 5. (A) Correlation between tyrosinase activity and total melanin (TM) content as the sum of eumelanin (EM) and pheomelanin (PM). Tyrosinase activities were measured by the in situ tyrosine hydroxylase assay. (B) Protein levels of tyrosinase by Western blotting. The sequence of cell cultures are in the order of tyrosinase activity given in (A), and the number corresponds to that shown in Figure 2 and Table 1 with the classification being shown in parentheses.

phenotype. It has been debated that human pigmentary phenotypes should be defined based on quantitative measures, rather than arbitrarily, such as the commonly

used Fitzpatrick's skin phototypes. The present study represents a step in the right direction, and analysis of additional melanocyte cultures should allow for classification according to EM and TM. In this study, we used a panel of cultured human melanocytes that were all maintained under identical culture conditions, as described in Materials and methods. All cultures were tested while in early passage (passages three to 10).

We found that EM, not PM, consistently increased with visual pigmentation. The ratio of EM/PM, as presented in the log value, varied widely, and sometimes was comparable in the dark (D+) and very light (L) melanocytes (Figure 3C). Nevertheless, we observed that on the average, lighter (L) melanocytes tend to be more pheomelanin in composition than darker (L+, D, and D+) melanocytes. Similar results have been reported for cultured human melanocytes (De Leeuw et al., 2001; Smit et al., 1998) and in isolated melanosomes thereof (van Nieuwpoort et al., 2004). These observations are consistent with our hypothesis proposed for mixed melanogenesis. We proposed that melanogenesis proceeds in three distinctive steps: cysteinyl-dopa-genes, pheomelanogenesis, followed by eumelanogenesis. It thus appears that the ratio of EM/PM is determined by tyrosinase activity and cysteine concentration (Chintala et al., 2005; Ito, 2003; Land and Riley, 2000).

Eumelanin, but not always PM, consistently correlates with the visual phenotype. This suggests that EM is more important in determining the degree of visual pigmentation in cultured human melanocytes. This may be attributable not only to the predominance of EM over PM but also to the relative effect on pigmentation. We have shown that absorbance of PM is much lower than that of EM: when dissolved in Soluene-350, 5-S-cysteinyl-dopa-melanin (PM) had an absorbance at 500 nm about 40% that of 5,6-dihydroxyindole-melanin (EM), and the difference was further accentuated in longer wavelengths (Ozeki et al., 1996). Our previous study, although preliminary, also showed that some melanoma cell lines with high PM contents did not have visible pigment (del Marmol et al., 1993).

Number ^b	MC1R genotype ^c	Classification	Log EM ^d ($\mu\text{g}/10^6$ cells)	Log PM ^d ($\mu\text{g}/10^6$ cells)	Log EM/PM ^d
Loss-of-function MC1R (n = 9) ^c					
1	V60L/V60L	L	-0.32	0.21	-0.53
2	R160W/R160W	L	-0.18	-0.37	0.18
18	R160W/+	L	0.54	0.79	-0.25
19	R160W/D294H	L	0.54	0.51	0.03
21	R142H/+	L	0.57	0.44	0.13
22	R160W/D294H	L	0.61	0.46	0.15
24	V60L/R160W	L	0.70	0.61	0.09
28	V60L/R160W	L	0.89	0.90	-0.01
32	R151C/D294H	L+	1.17	0.26	0.91
Functional MC1R (n = 10) ^c					
5	V92M/+	L	-0.08	-0.55	0.48
7	+/+	L	0.09	-0.14	0.24
8	R163Q/+	L	0.10	-0.36	0.46
10	R151C/+	L	0.14	-0.17	0.31
11	V60L/+	L	0.16	0.18	-0.01
15	V92M/V92M	L	0.41	0.03	0.38
30	+/+	L+	0.97	1.61	-0.64
38	+/+	L+	1.41	0.18	1.23
40	+/+	L+	1.43	0.33	1.10
41	+/+	L+	1.44	1.19	0.25

^aData for the following nine cultures were taken from Table 1 of Scott et al. (2002): nos 2, 5, 7, 8, 11, 15, 32, 38, and 40. The conversion factor of 5 for a sum of 4-AHP and 3-AHP was adapted in the present study (as in the original paper by Ito and Fujita, 1985) instead of 10 that was previously used in Scott et al. (2002) because it is consistent with the factor of 9 for 4-AHP (Wakamatsu and Ito, 2002).

^bThe number corresponds to the sequence presented in Table 1 and Figure 2.

^c+/+ = wild type MC1R; V60L, is weakly associated with red hair, V92M, and R163Q are considered 'pseudo alleles' with no significant effect on EM synthesis, while R151C, R160W, and D294H are strong red hair alleles. The function was assessed by the response to α -MSH as described by Scott et al. (2002) and Kadekaro et al. (2005).

^dNo significant differences in log EM, log PM, and log EM/PM values were found between the loss-of-function MC1R and the functional MC1R, by the Mann-Whitney nonparametric *U*-test: P-values are 0.343, 0.217, and 0.085, respectively.

Total melanin content, measured by HPLC, showed a good correlation with TM content measured spectrophotometrically (Figure 4). Similar correlations have been reported for human hair and skin samples (Alaluf et al., 2001; Ozeki et al., 1996).

In adult melanocyte cultures, the chemical phenotype correlated well with the ethnic background of the donors: Caucasian had the least, Indian had more, and African-American had the highest EM. A similar result has been obtained in our previous study in which cultured melanocytes from Caucasian donors had significantly less EM and PM compared with Asians (Hunt et al., 1995). It has been described that the in vivo differences in pigmentation of the skin remain evident in melanosomes isolated from cultured melanocytes (De Leeuw et al., 2001; van Nieuwpoort et al., 2004; Smit et al., 1998; Wenczl et al., 1998).

Another interesting finding with cultured adult melanocytes is that they contain significantly higher PM than cultured neonatal melanocytes. At present, the significance of higher PM levels in cultured adult melanocytes may be speculative (van Nieuwpoort et al., 2004;

Wenczl et al., 1998). Regarding the high PM levels, it should be pointed out that dysplastic nevus cells contain significantly more PM at the tissue (Salopek et al., 1991), cellular (Smit et al., 1998), and melanosomal level (Pavel et al., 2004). Dysplastic nevus cells are considered by some to be precursor lesions of melanoma (Bennett, 2003; Pavel et al., 2004).

In this study, tyrosinase activity measured as the tyrosine hydroxylase activity closely correlated directly with the TM content (Baker et al., 1995). The tyrosine hydroxylase assay is based on the release of tritium from the 3 and 5 positions of radiolabeled tyrosine in the form of tritiated water. Therefore, the method measures production of dopaquinone (release of 3-T) and the subsequent oxidative polymerization of dihydroxyindole monomers (release of 5-T) formed from dopaquinone and/or conversion to 5-S-cysteinyl-dopa (release of 5-T). Thus, it should be expected that this method reflect the degree of pigmentation.

The level of tyrosinase protein measured by the Western blotting only roughly paralleled the TM content. It is now clear that the expression of the regulatory

Table 2. Melanocortin-1 receptor (MC1R) genotype and eumelanin (EM) and pheomelanin (PM) contents in cultured human melanocytes^a

proteins, such as tyrosinase, is not the main determinant for the final TM or visual pigmentation. There are many other regulatory mechanisms that would determine protein activity, including post-translation modifications, availability at the proper microenvironment and so forth. Regarding tyrosinase, sorting and final anchoring to the melanosome is very important for its maximal function. Melanosomal pH appears to be another important regulation. It has been proposed that Caucasian melanocytes are acidic and thus pigmentation is suppressed both because of a lower tyrosinase activity and a lower rate of polymerization of melanin precursors at acidic pHs (Ancans et al., 2001; Hirobe et al., 2003; Smith et al., 2004).

Melanocortin-1 receptor is a transmembrane receptor located on the melanocytes. The binding of α -MSH or adrenocorticotropin to MC1R results in an increase of cAMP levels leading to the upregulation of tyrosinase and tyrosinase-related proteins (Abdel-Malek et al., 1995; Rees, 2003; Suzuki et al., 1996). Thus, loss-of-function mutations of MC1R leads to the switch to PM production in follicular melanocytes, giving rise to red hair in human (Naysmith et al., 2004) and yellow hair in mice (Ito and Wakamatsu, 2003; Ozeki et al., 1995). However, human skin had not been measured for melanin types in relation to *MC1R* mutation, and only one previous study addressed this issue in cultured human melanocytes (Scott et al., 2002). The study hereby presented represents a further attempt to measure EM and PM contents in human cultured melanocytes with known *MC1R* genotypes. We did not observe any significant differences in the log EM or log PM contents of the nine melanocyte cultures expressing loss-of-function *MC1R* compared with those of the 10 melanocyte cultures with functional *MC1R* (Table 2). Interestingly, one culture (no. 32) expressing two *MC1R* alleles known to be strongly associated with the RHC phenotype had a high EM (and a low PM). These observations confirm that expression of these *MC1R* alleles may not be enough for the fair skin phenotype and can be expressed in individuals with dark skin, as suggested by epidemiological studies (Kennedy et al., 2001; Matichard et al., 2004; Palmer et al., 2000). Our findings are consistent with previously reported results on the levels of tyrosinase and related proteins in *MC1R* genotyped primary melanocyte cultures from Queensland neonates, which showed no correlation of these pigmentation markers with *MC1R* genotype (Leonard et al., 2003). In fact, red haired individuals with black skin were recently identified in four Jamaicans having loss-of-function *MC1R* (McKenzie et al., 2003). The human *MC1R* gene is highly polymorphic and certain allelic variants of the gene are associated with the RHC phenotype, melanoma and non-melanoma skin cancer (Bastiaens et al., 2001; Kennedy et al., 2001; Palmer et al., 2000; Rees, 2003). Our previous study indicates that

loss-of-function mutations in the *MC1R* gene may not necessarily affect constitutive pigmentation, but predispose human melanocytes to the DNA damaging effects of UV radiation, which may increase melanoma risk (Kadekaro et al., 2005; Scott et al., 2002). From these considerations, it appears that *MC1R* mutations do not necessarily alter the skin phenotype but rather relate to increased sensitivity to UV-induced DNA damage.

Finally, the ratio of EM/PM varies tremendously regardless of degree of pigmentation in cultured melanocytes. It has been shown by Duval et al. (2002) that keratinocytes can strongly influence the EM/PM ratio for melanocytes in culture and also will play an important role for pigmentation regulation. It is also possible that regulation of levels of cysteine, a PM precursor, may account for the diversity of the ratio of EM/PM. In this regard, our recent study has demonstrated that *subtle gray (sut)* mouse pigmentation mutant arose by means of a mutation in the *Slc7a11* gene, encoding the plasma membrane cystine/glutamate exchanger xCT and a resulting low rate of extracellular cystine transport into *sut* melanocytes reduces PM production (Chintala et al., 2005). Thus, *Slc7a11* is a major genetic regulator of PM production in hair and melanocytes. It is conceivable that *Slc7a11* gene may be involved in the greater production of PM in some melanocyte cultures found in this study.

Conclusions

In conclusion, these results indicate that: (i) cultured human melanocytes vary tremendously in pigmentation; (ii) EM, but not always PM, consistently correlates with the visual phenotype; (iii) lighter melanocytes tend to be more pheomelanin in composition than darker melanocytes; (iv) in adult melanocyte cultures, EM correlates well with the ethnic background of the donors (African-American > Indian > Caucasian); and (v) *MC1R* loss-of-function mutations do not necessarily alter the phenotype of cultured melanocytes but rather relate to increased sensitivity to UV-induced DNA damage.

Materials and methods

Melanocytes culture

Primary human melanocyte cultures were established from fore-skins derived from anonymous newborn males ($n = 51$) or from skin biopsies ($n = 9$) obtained from the forearm or breast or abdomen tissue following surgery performed on young adults with known ethnic origin, after informed consent, and maintained as described (Abdel-Malek et al., 1995). Briefly, the culture medium consisted of MCDB 153, supplemented with 3% heat-inactivated fetal calf serum, 1% penicillin/streptomycin/amphotericin, 5 μ g/ml of insulin, 1 μ g/ml of α -tocopherol, 8 nM of TPA, 0.6 μ g/ml of basic fibroblast growth factor, and 13 μ g/ml of bovine pituitary extract. Early passage (<10) cultures were used for all experiments to insure minimal genetic drift in vitro. These cell cultures were

examined for visual pigmentation by microscopic observation and classified into four types: L, L+, D, and D+. The classification was made without prior knowledge of melanin contents by HPLC assays and spectrophotometry.

Analysis of EM and PM and spectrophotometric TM content

Melanocytes were lyophilized and $0.2\text{--}0.5 \times 10^6$ cells each were processed for chemical analyses of EM to detect the specific degradation product, pyrrole-2,3,5-tricarboxylic acid (PTCA), after permanganate oxidation (Ito and Fujita, 1985; Ito and Wakamatsu, 1994) and of PM to detect the specific degradation product, 4-amino-3-hydroxyphenylalanine (4-AHP), after hydriodic acid hydrolysis (Ito and Fujita, 1985; Wakamatsu and Ito, 2002). The amounts of EM was obtained by multiplying the PTCA value by a conversion factor of 160 (Ozeki et al., 1996), while the amount of PM was obtained by multiplying the 4-AHP value by a conversion factor of 9 (Wakamatsu and Ito, 2002). The PTCA determinations were performed in duplicate and the 4-AHP determinations were as single measurements. Some data ($n = 15$) for PM were obtained with our previous method analyzing a combined amount of 4-AHP and 3-amino-4-hydroxyphenylalanine (3-AHP) and a conversion factor of 5 (Ito and Fujita, 1985). For spectrophotometric analysis of TM content, the cells were harvested and counted, and 1×10^6 melanocytes were lysed using 1% Triton-X. Lipid from the cell lysates were removed using an ethanol:ether (1:1) solution. Purified melanin pellets were resuspended in 0.2 M NaOH (1×10^6 cells/ml) and samples were heated at 60°C to solubilize the melanin. Absorbance of the samples was determined at 490 nm using a Bio-Rad Microplate Reader (Model 550; Bio-Rad, Hercules, CA, USA). Melanin content was determined using a standard curve generated from known concentrations of synthetic melanin (Sigma, St. Louis, MO, USA).

Determination of tyrosinase activity

To determine the in situ tyrosine hydroxylase activity of tyrosinase (Abdel-Malek et al., 1992; Pomeranz, 1969), melanocytes were plated onto 60 mm dishes at a density of 2.5×10^5 cells. After 72 h, cells were incubated in the presence of tritium labeled tyrosine for 24 h, and the amount of tritium labeled water that was released by the cells into the media was measured. For each culture, triplicate dishes and two determinations per dish were analyzed.

Immunoblot analysis of tyrosinase

Human melanocytes were plated onto 100 mm dishes at a density of 1.5×10^6 cells. Seventy-two hours later cell extracts were prepared using radioimmunoprecipitation assay buffer containing a cocktail of protease inhibitors. Twelve micrograms of each cell lysate was used for electrophoresis in a 10% polyacrylamide gel. The separated proteins were transblotted onto Immobilon-P membranes that were incubated with the α -hPEP-7 (1:10 000 dilution), a polyclonal antibody raised against the carboxy-terminus of the human tyrosinase (from Richard King and William Oetting, University of Minnesota, Minneapolis, MN, USA), for 18 h at 4°C, followed by incubation with horseradish peroxidase-conjugated anti-mouse IgG at 1:1000 dilution, for 1 h at room temperature. Membranes were also reacted with horseradish peroxidase-conjugated actin antibody at 1:500 dilution, as control for loading. The bands were visualized using Enhanced Chemiluminescence (Amersham, Arlington Heights, IL, USA) according to the manufacturer's instructions.

Sequencing of MC1R gene

Total RNA was isolated from cultured human melanocytes using the RNA Easy Kit (Qiagen Science, Valencia, CA, USA) and cDNA

was obtained by reverse transcription of 100 ng of total RNA using random hexamers as primers (50 μ M Oligo(dT)/20 μ l final volume). An equivalent volume of 2 μ l of cDNA suspension was used for RT-PCR amplification using SuperScript TMIII, Invitrogen Life Technologies (Carlsbad, CA, USA). The entire coding region of the *MC1R* was amplified in two separate reactions using the following sets of primers: for the first-half of the sequence N-terminal primer (5'-GCAGCACCATGAACTAAGCA-3') and C-terminal primer (5'-CCAGCATAGCCAGGAAGAAG-3') and for the second-half of the sequence N-terminal primer (5'-GTGGACCGCCTACATCCAT-3') and C-terminal primer (5'-GGACCAGGGAGGTAAGGAAC-3'). A PCR touchdown cycling profile was used, consisting of one cycle of 95°C for 5 min, followed by 25 cycles of 94°C for 1 min, 62°C for 1 min with a 0.5°C/cycle decrease, and 72°C for 1 min; followed by 10 cycles of 94°C for 1 min, 55°C for 1 min, 72°C for 1 min, and a final extension at 72°C for 10 min. The PCR products were purified with a QIAquick PCR Purification Kit (Qiagen Science) according to the manufacturer's instructions and sequenced with an automated system (Perkin Elmer/Applied Biosystems instrument models 373A or 377; Perkin Elmer/Applied Biosystems, Boston, MA, USA). For some cultures, the *MC1R* genotyping was carried out using 25–50 ng of genomic DNA, as described by Duffy et al. (2004).

Statistical analysis

Statistical testing was carried out using JMP 5.0 for Macintosh (SAS Institute, Japan: <http://www.jmp.com/japan/corp/index.shtml>). Differences were analyzed for statistical significance using the Mann-Whitney nonparametric *U*-test. $P < 0.05$ are considered to be significant.

Acknowledgements

This study was supported in part, by a grant-in-aid for Scientific Research (no. 16591122) from the Ministry of Education, Culture, Sports and Technology of Japan (K. Wakamatsu and S. Ito); by RO1 ES-09110 and ES06096 (Z. Abdel-Malek), Johnson & Johnson Skin Research Center Training grant (A.L. Kadekar and Z. Abdel-Malek), and by Dermatology Foundation Research Grant (S. Leachman).

References

- Abdel-Malek, Z., Swope, V.B., Pallas, J., Krug, K., and Nordlund, J.J. (1992). Mitogenic, melanogenic and cAMP responses of cultured neonatal human melanocytes to commonly used mitogens. *J. Cell. Physiol.* **150**, 416–425.
- Abdel-Malek, Z., Swope, V.B., Suzuki, I., Akcali, C., Harriger, M.D., Boyce, S.T., Urabe, K., and Hearing, V.J. (1995). Mitogenic and melanogenic stimulation of normal human melanocytes by melanotropic peptides. *Proc. Natl Acad. Sci. U.S.A.* **92**, 1789–1793.
- Alaluf, S., Heath, A., Carter, N., Atkins, D., Mahalingam, H., Barrett, K., Kolb, R., and Smit, N. (2001). Variation in melanin content and composition in type V and VI photoexposed and photoprotected human skin: the dominant role of DHI. *Pigment Cell Res.* **14**, 337–347.
- Alaluf, S., Atkins, D., Barrett, K., Blount, M., Carter, N., and Heath, A. (2002). The impact of epidermal melanin on objective measurements of human skin colour. *Pigment Cell Res.* **15**, 119–126.
- Ancans, J., Tobin, D.J., Hoogdujin, M.J., Smit, N.P., Wakamatsu, K., and Thody, A.J. (2001). Melanosomal pH controls rate of melanogenesis, eumelanin/phaeomelanin ratio and melanosome maturation in melanocytes and melanoma cells. *Exp. Cell Res.* **268**, 26–35.

- Baker, D., Dixon, K., Medrano, E.E., Smalara, D., Im, S., Mitchell, D., Babcock, G., and Abdel-Malek, Z.A. (1995). Comparison of the responses of human melanocytes with different melanin contents to ultraviolet B irradiation. *Cancer Res.* **55**, 4041–4046.
- Bastiaens, M.T., ter Huurne, J.A., Kielich, C., Gruis, N.A., Westendorp, R.G., Vermeer, B.J., Bavinck, J.N., and Leiden Skin Cancer Study Team (2001). Melanocortin-1 receptor gene variants determine the risk of nonmelanoma skin cancer independently of fair skin and red hair. *Am. J. Hum. Genet.* **68**, 884–894.
- Beaumont, K.A., Newton, R.A., Smit, D.J., Leonard, J.H., Stow, J.L., and Sturm, R.A. (2005). Altered cell surface expression of human MC1R variant receptor alleles associated with red hair and skin cancer risk. *Hum. Mol. Genet.* **14**, 2145–2154.
- Bennett, D.C. (2003). Human melanocyte senescence and melanoma susceptibility genes. *Oncogene* **22**, 3063–3069.
- Chintala, S., Li, W., Lamoreux, M.L. et al. (2005). *Slc7a11* gene controls production of pheomelanin pigment and proliferation of cultured cells. *Proc. Natl Acad. Sci. USA* **102**, 10964–10969.
- De Leeuw, S.M., Smit, N.P.M., Van Veldhoven, M., Pennings, E.M., Pavel, S., Simons, W.I.M., and Schothorst, A.A. (2001). Melanin content of cultured human melanocytes and UV-induced cytotoxicity. *J. Photochem. Photobiol. B, Biol.* **61**, 106–113.
- Duffy, D.L., Box, N.F., Chen, W., Palmer, J.S., Montgomery, G.W., James, M.R., Hayward, N.K., Martin, N.G., and Sturm, R.A. (2004). Interactive effects of MC1R and OCA2 on melanoma risk phenotypes. *Hum. Mol. Genet.* **13**, 447–461.
- Duval, C., Smit, N.P.M., Kolb, A.M., Régnier, M., Pavel, S., and Schmidt, R. (2002). Keratinocytes control the pheo/eumelanin ratio in cultured normal human melanocytes. *Pigment Cell Res.* **15**, 440–446.
- García-Borrón, J.C., Sánchez-Laorden, B.L., and Jiménez-Cervantes, J. (2005). Melanocortin-1 receptor structure and functional regulation. *Pigment Cell Res.* **18**, 393–410.
- Hearing, V.J. (1998). The regulation of melanin production. In *The Pigmentary System: Physiology and Pathophysiology*, J.J. Nordlund, R. Boissy, V.J. Hearing, R.A. King, J.-P. Ortonne, eds (New York: Oxford University Press), pp. 423–438.
- Hennessy, A., Oh, C., Diffey, B., Wakamatsu, K., Ito, S., and Rees, J. (2005). Eumelanin and pheomelanin concentrations in human epidermis before and after UVB irradiation. *Pigment Cell Res.* **18**, 220–223.
- Hirobe, T., Wakamatsu, K., and Ito, S. (2003). Changes in the proliferation and differentiation of neonatal mouse pink-eyed dilution melanocytes in the presence of excess tyrosine. *Pigment Cell Res.* **16**, 619–628.
- Hunt, G., Kyne, S., Ito, S., Wakamatsu, K., Todd, C., and Thody, A.J. (1995). Eumelanin and pheomelanin contents of human epidermis and cultured melanocytes. *Pigment Cell Res.* **8**, 202–208.
- Ito, S. (1997). Advances in chemical analysis of melanins. In *The Pigmentary System: Physiology and Pathophysiology*, J.J. Nordlund, R.E. Boissy, V.J. Hearing, R.A. King, and J.P. Ortonne, eds (New York: Oxford University Press), pp. 439–450.
- Ito, S. (2003). A chemist's view of melanogenesis. *Pigment Cell Res.* **16**, 230–236.
- Ito, S., and Fujita, K. (1985). Microanalysis of eumelanin and pheomelanin in hair and melanomas by chemical degradation and liquid chromatography. *Anal. Biochem.* **144**, 523–536.
- Ito, S., and Wakamatsu, K. (1994). An improved modification of permanganate oxidation of eumelanin that gives a constant yield of pyrrole-2,3,5-tricarboxylic acid. *Pigment Cell Res.* **7**, 141–144.
- Ito, S., and Wakamatsu, K. (2003). Quantitative analysis of eumelanin and pheomelanin in humans, mice, and other animals: a comparative review. *Pigment Cell Res.* **16**, 523–531.
- Kadekaro, A.L., Kavanagh, R., Kanto, H. et al. (2005). α -Melanocortin and endothelin-1 activate antiapoptotic pathways and reduce DNA damage in human melanocytes. *Cancer Res.* **65**, 4292–4299.
- Kennedy, C., Ter Huurne, J., Berkhout, M., Gruis, N., Bastiaens, M., Bergman, W., Willemze, R., and Bowes Bavinck, J.N. (2001). Melanocortin 1 receptor (*MC1R*) gene variants are associated with an increased risk for cutaneous melanoma which is largely independent of skin type and hair color. *J. Invest. Dermatol.* **117**, 294–300.
- Land, E., and Riley, P.A. (2000). Spontaneous redox reactions of dopaquinone and the balance between eumelanin and pheomelanin pathways. *Pigment Cell Res.* **13**, 273–277.
- Leonard, J.H., Marks, L.H., Chen, W., Cook, A.L., Boyle, G.M., Smit, D.J., Brown, D.L., Stow, J.L., Parsons, P.G., and Sturm, R.A. (2003). Screening of human primary melanocytes of defined melanocortin-1 receptor genotype: pigmentation marker, ultrastructural and UV-survival studies. *Pigment Cell Res.* **16**, 198–207.
- Liu, Y., Hong, L., Wakamatsu, K., Ito, S., Adhyaru, B.B., Cheng, C.Y., Bowers, C.R., and Simon, J.D. (2005). Comparisons of the structural and chemical properties of melanosomes isolated from retinal pigment epithelium, iris and choroids of newborn and mature bovine eyes. *Photochem. Photobiol.* **81**, 510–516.
- del Marmol, V., Ito, S., Jackson, I., Vachtenheim, J., Berr, P., Ghannem, G., Morandini, R., Wakamatsu, K., and Huez, G. (1993). TRP-1 expression correlates with eumelanogenesis in human pigment cells in culture. *FEBS Lett.* **327**, 307–310.
- Matichard, E., Verpillat, P., Meziani, R. et al. (2004). Melanocortin 1 receptor (*MC1R*) gene variants may increase the risk of melanoma in France independently of clinical risk factors and UV exposure. *J. Med. Genet.* **41**, e13.
- McKenzie, C.A., Harding, R.M., Brown Tomlinson, J., Ray, A.J., Wakamatsu, K., and Rees, J.L. (2003). Phenotypic expression of melanocortin-1 receptor mutations in black Jamaicans. *J. Invest. Dermatol.* **121**, 207–208.
- Naysmith, L., Waterston, K., Ha, T., Flanagan, N., Bisset, Y., Ray, A., Wakamatsu, K., Ito, S., and Rees, J. L. (2004). Quantitative measures of the effect of the melanocortin 1 receptor on human pigmentation status. *J. Invest. Dermatol.* **122**, 423–428.
- van Nieuwpoort, F., Smit, N.P.M., Kolb, R., van der Meulen, H., Koerten, H., and Pavel, S. (2004). Tyrosine-induced melanogenesis shows differences in morphologic and melanogenic preferences of melanosomes from light and dark skin types. *J. Invest. Dermatol.* **122**, 1251–1255.
- Ozeki, H., Ito, S., Wakamatsu, K., and Hirobe, T. (1995). Chemical characterization of hair melanins in various coat-color mutants of mice. *J. Invest. Dermatol.* **105**, 361–366.
- Ozeki, H., Ito, S., Wakamatsu, K., and Thody, A.J. (1996). Spectrophotometric characterization of eumelanin and pheomelanin in hair. *Pigment Cell Res.* **9**, 265–270.
- Palmer, J.S., Duffy, D.L., Box, N.F., Aitken, J.F., O'gorman, L.E., Green, A.C., Hayward, N.K., Martin, N.G., and Sturm, R.A. (2000). Melanocortin-1 receptor polymorphisms and risk of melanoma: is the association explained solely by pigmentation phenotype? *Am J. Hum. Genet.* **66**, 176–186.
- Pavel, S., van Nieuwpoort, F., van der Meulen, H., Out, C., Pizinger, K., Cetkovská, P., Smit, N.P.M., and Koerten, H.K. (2004). Disturbed melanin synthesis and chronic oxidative stress in dysplastic naevi. *Eur. J. Cancer* **40**, 1423–1430.
- Pomeranz, S.H. (1969). L-tyrosine-3,5-³H assay for tyrosinase development in skin of newborn hamsters. *Science* **164**, 838–839.
- Prota, G. (1992). *Melanin and Melanogenesis* (New York: Academic Press), pp. 1–290.
- Rees, J.L. (2003). Genetics of hair and skin color. *Ann. Rev. Genet.* **37**, 67–90.

Wakamatsu et al.

- Salopek, T.G., Yamada, K., Ito, S., and Jimbow, K. (1991). Dysplastic melanocytic nevi contain high levels of pheomelanin: quantitative comparison of pheomelanin/eumelanin levels between normal skin, common nevi, and displastic nevi. *Pigment Cell Res.* 4, 172–178.
- Scott, M.C., Wakamatsu, K., Ito, S. et al. (2002). Human melanocortin receptor variants, receptor function and melanocyte response to UV radiation. *J. Cell Sci.* 115, 2349–2355.
- Smit, N.P.M., Kolb, R.M., Lentijes, E.G.W.M., Noz, K.C., van der Meulen, H., Koerten, H.K., Vermeer, B.J., and Pavel, S. (1998). Variations in melanin formation by cultured melanocytes from different skin types. *Arch. Dermatol. Res.* 290, 342–349.
- Smith, D.R., Spaulding, D.T., Glenn, H.M., and Fuller, B.B. (2004). The relationship between Na⁺/H⁺ exchanger expression and tyrosinase activity in human melanocytes. *Exp. Cell Res.* 298, 521–534.
- Suzuki, I., Cone, R., Im, S., Nordlund, J., and Abdel-Malek, Z. (1996). Binding of melanotropic hormones to the melanocortin receptor MC1R on human melanocytes stimulates proliferation and melanogenesis. *Endocrinology* 137, 1627–1633.
- Wakamatsu, K., and Ito, S. (2002). Advanced chemical methods in melanin determination. *Pigment Cell Res.* 15, 174–177.
- Wenczl, E., Van der Schans, G.P., Roza, L., Kolb, R.M., Timmerman, A.J., Smit, N.P.M., Pavel, S., and Schorthorst, A.A. (1998). (Pheo)melanin photosensitizes UVA-induced DNA damage in cultured human melanocytes. *J. Invest. Dermatol.* 111, 678–682.

Determination of eumelanin in human urine

Kazumasa Wakamatsu^{1*}, Akihiko Takasaki²,
Bertil Kågedal³, Toshiro Kageshita⁴ and
Shosuke Ito¹

¹Department of Chemistry, Fujita Health University School of Health Sciences, Toyoake, Aichi, Japan

²Clinical Hematology, Fujita Health University School of Health Sciences, Toyoake, Aichi, Japan

³Department of Biomedicine and Surgery, Division of Clinical Chemistry, Linköping University, Linköping, Sweden

⁴Department of Dermatology, Kumamoto University School of Medicine, Kumamoto, Japan

*Address correspondence to Kazumasa Wakamatsu,
e-mail: kwaka@fujita-hu.ac.jp

Summary

Normal and malignant melanocytes produce melanins and melanin-related metabolites, most of which are retained in the cells but some are secreted into the blood and then excreted in the urine. In this study, we developed a method to measure levels of eumelanin in urine samples and evaluated its clinical significance in comparison with the melanin-related metabolites 6-hydroxy-5-methoxyindole-2-carboxylic acid (6H5MI2C) and 5-S-cysteinyl-dopa (5-S-CD), and with pheomelanin, measured after degradation as 4-amino-3-hydroxy-phenylalanine (4-AHP). The method is based on the production of pyrrole-2,3,5-tricarboxylic acid (PTCA) on permanganate oxidation of eumelanin, followed by quantification by liquid chromatography. For 118 urine samples from 10 control subjects, mean urinary excretions of PTCA, 6H5MI2C, 5-S-CD and 4-AHP were 19, 67, 37 and 59 $\mu\text{mol/mol}$ creatinine respectively. In melanoma patients ($n = 45$), the mean urinary excretions of PTCA, 6H5MI2C, 5-S-CD, and 4-AHP were 91, 926, 4070 and 3530 $\mu\text{mol/mol}$ creatinine respectively. Median level of PTCA in melanoma patients was elevated 2.1-fold compared with control subjects. The degrees of elevation for 6H5MI2C, 5-S-CD, and 4-AHP were 1.8-, 22- and 6.2-fold respectively. Thus, although urinary PTCA is of little clinical value in following the progression of melanoma, urinary 4-AHP appears to be of considerable value in this respect.

Key words: 5-S-cysteinyl-dopa/eumelanin/6-hydroxy-5-methoxyindole-2-carboxylic acid/melanoma/pheomelanin/serum/urine

Received 22 February 2005, revised and accepted for publication 12 September 2005

Introduction

Normal melanocytes as well as their malignant derivatives, the melanoma cells, produce melanins and melanin-related metabolites, most of which are retained in the cells but some are secreted into the blood and then excreted into the urine. It is thus expected that the levels of these melanin-related compounds in serum or urine may reflect the degree of pigmentation (Ekelund et al., 1985; Westerhof et al., 1987) and the progression of melanoma (Hartleb and Arndt, 2001).

The production of melanin pigment is catalyzed by the specific enzyme tyrosinase, which converts L-tyrosine to dopaquinone (Hearing, 1998; Ito, 2003). Dopaquinone is a highly reactive molecule, and in the absence of sulfhydryl compounds, it gives rise to dopachrome through rapid cyclization and redox reactions. Dopachrome is then either decarboxylated to give 5,6-dihydroxyindole (DHI) or tautomerized to give 5,6-dihydroxyindole-2-carboxylic acid (DHICA). DHI and DHICA are then oxidized to form eumelanin, a dark brown to black pigment. However, a significant portion of DHICA leaks into the blood stream and is excreted in the urine after O-methylation to the isomeric compounds 5-hydroxy-6-methoxyindole-2-carboxylic acid (5H6MI2C) and 6-hydroxy-5-methoxyindole-2-carboxylic acid (6H5MI2C; Wakamatsu et al., 1990; Westerhof et al., 1987). These indolic eumelanin metabolites are considered to reflect tyrosinase activity in normal melanocytes and melanoma cells (Ekelund et al., 1985; Wakamatsu et al., 1990; Westerhof et al., 1987). In fact, urinary excretion of 6H5MI2C has been evaluated as a marker of melanoma progression (Yamada et al., 1992).

In the presence of cysteine, however, dopaquinone rapidly reacts with cysteine to form 5-S-cysteinyl-dopa (5-S-CD) along with minor amounts of cysteinyl-dopa isomers (Ito, 2003). Oxidation of cysteinyl-dopa isomers in melanocytes leads to the production of pheomelanin, a yellow to reddish melanin, but a significant portion of cysteinyl-dopa escapes from melanocytes, especially melanoma cells (Wakamatsu et al., 1990). It is thus possible to estimate the progression of melanoma by measuring the concentration of 5-S-CD in the blood or urine (Agrup et al., 1979; Hartleb and Arndt, 2001;

Horikoshi et al., 1994; Kärnell et al., 2000; Wakamatsu et al., 2002c).

We have recently shown that in addition to 6H5MI2C and 5-S-CD, melanoma patients secrete high levels of pheomelanin into the blood and urine (Takasaki et al., 2003; Wakamatsu et al., 2003). The measurement of pheomelanin is based on the formation of 4-amino-3-hydroxyphenylalanine (4-AHP) on reductive hydrolysis of pheomelanin with hydriodic acid (Ito and Fujita, 1985; Wakamatsu et al., 2002b). Serum pheomelanin level was found to be elevated in metastatic melanoma patients but is less sensitive than serum 5-S-CD in indicating presence of distant metastases (Wakamatsu et al., 2003). However, no report has appeared measuring the concentration of eumelanin in blood or urine from melanoma patients.

Eumelanin can be analysed by permanganate oxidation to the specific degradation product, pyrrole-2,3,5-tricarboxylic acid (PTCA; Ito and Fujita, 1985) followed by quantitation of PTCA by high performance liquid chromatography (HPLC). In the present study, we applied this specific HPLC method to measure eumelanin (PTCA) in urine samples and evaluated its clinical significance in melanoma. We examined the correlation of PTCA to the melanin-related metabolites 6H5MI2C and 5-S-CD and to pheomelanin (as quantified by the analysis of the degradation product 4-AHP) in melanoma patients as well as control subjects and compared the increase of urinary PTCA levels in melanoma patients with those of the other melanoma markers. We also evaluated the clinical significance of PTCA levels in serum in a limited number of melanoma cases.

Results

Method for determining urinary levels of eumelanin (PTCA)

To determine urinary levels of eumelanin, we intended to use principally the same method as used for eumelanin analyses in hairs, skins or cells (Wakamatsu and Ito, 2002a). However, in early trials to develop the method, we encountered difficulty in separating the PTCA peaks from interfering, large peaks in HPLC chromatogram. This difficulty was overcome by shifting to a chromatographic column with improved selectivity and the change of column temperature (see the Materials and methods). Figure 1 shows typical chromatograms of a standard and KMnO_4 oxidation products of urine samples from a control subject and from a melanoma patient. Pyrrole-2,3,5-tricarboxylic acid peaks were well separated from other peaks, despite of the fact that the peaks were small in most cases. In order to examine whether the small peaks were in fact PTCA or not, we collected the peak fraction with the same retention time as PTCA in HPLC and performed Liquid chromatography/mass spectrometry/mass spectrometry (LC/MS/MS) analysis. We observed the $[\text{M-H}]^+$ (m/z 198.1) peak

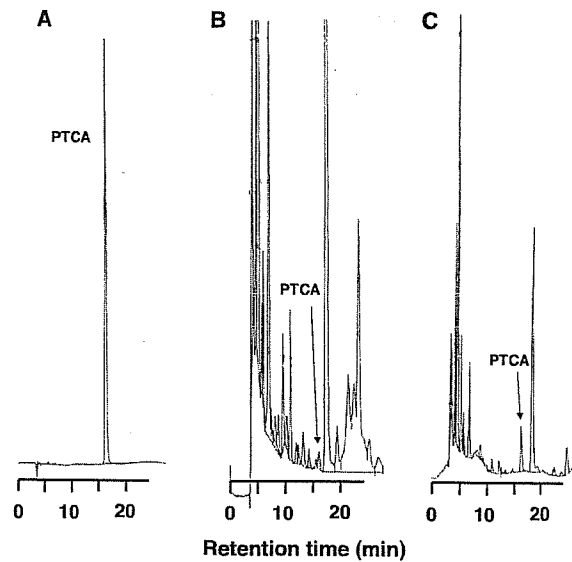


Figure 1. HPLC chromatograms of standard and permanganate oxidation products. (A) Standard of PTCA. Injected amount 91 ng. Sensitivity: 32 mV/full scale. (B) Oxidation product of urine sample from a control subject. Urinary PTCA level is 124 nmol/l. Sensitivity: 8 mV/full scale. (C) Oxidation products of urine sample from a melanoma patient. Urinary PTCA level is 1330 nmol/l. Sensitivity: 32 mV/full scale.

corresponding to PTCA, and $[\text{M-H-H}_2\text{O}]^+$ (m/z 180.0), $[\text{M-H-CO}_2]^+$ (m/z 154.1) and $[\text{M-H-2CO}_2]^+$ (m/z 110.1) peaks, which correspond to product ions as proved by the MS/MS spectrum, and thus the HPLC peak with the same retention time as the standard PTCA was identified as PTCA.

The possibility that ordinary urinary components might affect the recovery of PTCA was examined by adding *Sepia* melanin to a pooled urine sample. The recovery of PTCA after permanganate oxidation was $8.0 \pm 1.6 \mu\text{g}/\text{mg}$ *Sepia* melanin ($n = 5$), which is similar to reported values (Liu et al., 2004). This indicates that urinary components do not affect the yield of PTCA.

Comparison of urinary PTCA, 6H5MI2C, 5-S-CD, and 4-AHP between control subjects and melanoma patients

Figure 2 shows the excretions of PTCA, 6H5MI2C, 5-S-CD, and 4-AHP in urine from control subjects and Swedish melanoma patients. The data are positively skewed and are therefore shown in logarithmic scales. The median excretions are given in the figure, and the arithmetic means \pm SD are given below.

For the 118 samples from 10 control subjects, the urinary mean levels of PTCA, 6H5MI2C, 5-S-CD and 4-AHP were 19 ± 19 , 67 ± 54 , 37 ± 28 and $59 \pm 36 \mu\text{mol}/\text{mol}$ creatinine respectively.

Levels of urinary PTCA showed a seasonal variation (Figure 3). The highest value of $39 \pm 12 \mu\text{mol}/\text{mol}$

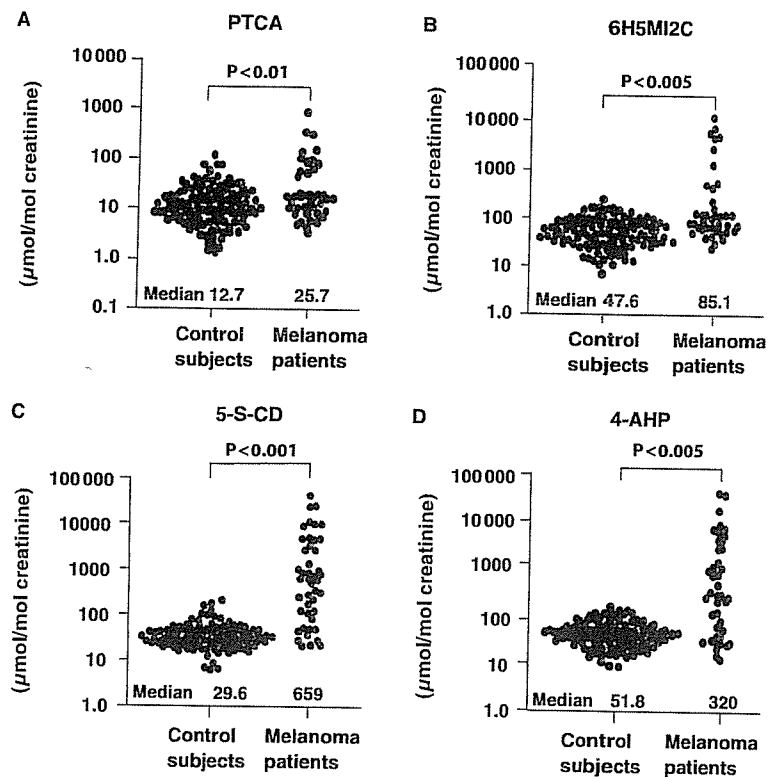


Figure 2. Distribution of urinary levels of (A) PTCA, (B) 6H5MI2C, (C) 5-S-CD, (D) 4-AHP in control subjects and in melanoma patients. Values are expressed in $\mu\text{mol}/\text{mol}$ creatinine.

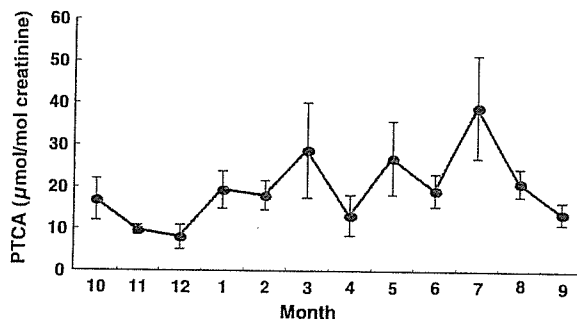


Figure 3. Seasonal variation of urinary levels of PTCA in control subjects. The data are expressed as mean \pm SE.

creatinine was found in July and the lowest value of $8.9 \pm 2.4 \mu\text{mol}/\text{mol}$ creatinine in December ($P < 0.001$). Each subject showed a large fluctuation in urinary levels of PTCA in the course of the 1-yr period.

For the 45 urine samples from Swedish melanoma patients, urinary levels of PTCA, 6H5MI2C, 5-S-CD and 4-AHP were 91 ± 185 , 926 ± 2160 , 4070 ± 8690 and $3530 \pm 8550 \mu\text{mol}/\text{mol}$ creatinine respectively.

The median urinary level of PTCA in melanoma patients was significantly elevated 2.1-fold compared with control subjects. Likewise, the median levels of 6H5MI2C, 5-S-CD, and 4-AHP in melanoma patients were significantly elevated 1.8-, 22-, and 6.2-fold compared with control subjects respectively.

Correlations between urinary levels of PTCA, 6H5MI2C, 5-S-CD, and 4-AHP

Correlation coefficients (r^2) between the four markers are summarized in Table 1. In control urine, statistically significant correlation was not found among the four markers. In the urine of Swedish melanoma patients, the pair 5-S-CD and 4-AHP showed the highest coefficient, followed by the pair 6H5MI2C and PTCA when calculated on logarithmic data (logarithmic data are more insensitive to extreme values than linear data). These correlations were expected because of the relations between 5-S-CD and 4-AHP in pheomelanin biosynthesis and between 6H5MI2C and PTCA in eumelanin biosynthesis. A high correlation of linear data was obtained between PTCA and 5-S-CD because three samples with high values of PTCA and 5-S-CD lay closely on the same regression line.

Contents of eumelanin and pheomelanin can be calculated with conversion factors of 160 g eumelanin/g PTCA (Ozeki et al., 1996) and 9 g pheomelanin/g 4-AHP (Wakamatsu et al., 2002b), the molecular weight of 199 for PTCA and the molecular weight of 196 for AHP. Figure 4 shows a relation of linear data between urinary levels of eumelanin and pheomelanin in the Swedish melanoma patients. In 27 (60%) of the 45 Swedish melanoma cases, the excretion of pheomelanin was found to be higher than the excretion of eumelanin. On the average, these melanoma patients excreted twice as